

SUMMARY REPORT

on

STUDY TO DETERMINE EXPERIMENTALLY THE
FEASIBILITY OF NEW METHODS FOR IMPROVING
THERMAL CONDUCTANCE OF MECHANICAL JOINTS
IN A VACUUM

to

GEORGE C. MARSHALL SPACE FLIGHT CENTER
NATIONAL AERONAUTICS AND SPACE ADMINISTRATION

December 15, 1966

NAS 8-20328

by

C. L. Coffin, F. A. Creswick, and J. E. Sorenson

BATTELLE MEMORIAL INSTITUTE
Columbus Laboratories
505 King Avenue
Columbus, Ohio 43201

TABLE OF CONTENTS

	<u>Page</u>
SUMMARY	2
CONCLUSIONS	3
RECOMMENDATIONS	4
EXPERIMENTAL PROCEDURE	4
Test-Specimen Design Considerations	5
Specimen-Material Selection	5
Rigid-Surface Specimen Design	5
Surface-Plateauing Procedures	5
Mechanical-Friction Plateauing Methods	6
Ultrasonic-Vibration Methods	6
Electric-Heating Methods	11
Hydrostatic-Fluid Thermal-Conductivity Measurement	11
Machined-Surface Characteristics	13
FLEXIBLE-SURFACE DIAPHRAGM DESIGN	14
DISCUSSION OF PROGRAM RESULTS	14
Search for Thermally Conductive Fluids	14
Silicone Fluid/Metal-Particle Slurries	17
Liquid Metals	17
General Considerations	19
Plateauing Investigation	19
Mechanical Plateauing	19
Ultrasonic-Vibration Plateauing	20
Pulsed Heating	23
Lapped Surface	25
Electric Discharge Machining	25
General Considerations	25
Diaphragm Effectiveness	29
REFERENCES	32
BIBLIOGRAPHY	33
APPENDIX A	
FLEXIBLE SURFACE DIAPHRAGM THICKNESS, EQUATION DERIVATION AND DESIGN COMPUTATION	A-1
APPENDIX B	
EFFECTIVENESS OF DIAPHRAGM IN TRANSFERRING HEAT, NEGLECTING THE CONDUCTANCE OF THE PRESSURIZING HYDROSTATIC FLUID OR PASTE, EQUATION DERIVATION AND EXAMPLE COMPUTATION	B-1
NOMENCLATURE	

LIST OF FIGURES

	<u>Page</u>
FIGURE 1. DEVICE USED TO IMPART TRANSLATORY RELATIVE MOTION TO RIGID SURFACES FOR THE PLATEAUIING STUDIES	7
FIGURE 2. RIGID-SURFACE SPECIMEN-PAIR SETUP FOR AN EXPERIMENT	8
FIGURE 3. LATHE SETUP WITH ULTRASONIC TRANSDUCER USED FOR AXIAL-RELATIVE-MOTION ULTRASONIC-VIBRATION TESTS	9
FIGURE 4. FIXTURE SETUP WITH ULTRASONIC TRANSDUCER USED FOR TRANSLATORY RELATIVE MOTION ULTRASONIC VIBRATION TESTS	10
FIGURE 5. APPARATUS FOR MEASURING HYDROSTATIC FLUID THERMAL CONDUCTIVITY	12
FIGURE 6. SCHEMATIC DIAGRAM OF FLEXIBLE SURFACE DIAPHRAGM AND MATING SURFACE	15
FIGURE 7. TYPICAL SURFACE WAVINESS PROFILE USED FOR THE FLEXIBLE SURFACE DIAPHRAGM DESIGN	16
FIGURE 8. SEVERE GALLING DAMAGE OF ALUMINUM SURFACES CAUSED BY RELATIVE MOTION WITH SPECIMEN SURFACES DRY	21
FIGURE 9. SEVERE GALLING DAMAGE OF ALUMINUM SURFACES CAUSED BY RELATIVE MOTION WITH SPECIMEN SURFACES LUBRICATED WITH KEROSENE	21
FIGURE 10. LIGHT GALLING DAMAGE OF ALUMINUM AND STAINLESS STEEL SURFACES CAUSED BY RELATIVE MOTION WITH SPECIMEN SURFACES DRY	22
FIGURE 11. LIGHT GALLING DAMAGE OF ALUMINUM AND STAINLESS STEEL SURFACES CAUSED BY RELATIVE MOTION WITH SPECIMEN SURFACES LUBRICATED WITH KEROSENE	22
FIGURE 12. TALYSURF CHART SHOWING APPARENT SMOOTHING EFFECT OF ULTRASONIC VIBRATION IN A REGION OF A MILD STEEL SURFACE	24
FIGURE 13. TALYSURF CHART SHOWING APPARENT SMOOTHING EFFECT IN A REGION OF A STAINLESS STEEL SURFACE	24
FIGURE 14. GALLING AND PITTING DAMAGE OF ALUMINUM SURFACES CAUSED BY RELATIVE MOTION WITH ELECTRIC CURRENT PULSE HEATING, WITH SPECIMEN SURFACES DRY	26
FIGURE 15. GALLING AND PITTING DAMAGE OF ALUMINUM AND STAINLESS STEEL SURFACES CAUSED BY RELATIVE MOTION WITH ELECTRIC CURRENT PULSE HEATING, WITH SPECIMEN SURFACES DRY	26
FIGURE 16. TALYSURF CHARTS SHOWING APPARENT SLIGHT SMOOTHING EFFECT OF ELECTRIC CURRENT PULSE HEATING AN ALUMINUM SURFACE WITH A PRESSED GRAPHITE TOOL	27

LIST OF FIGURES (Continued)

	<u>Page</u>
FIGURE 17. TALYSURF CHART SHOWING ALUMINUM SURFACE LAPPED WITH A FINE-GRIT COMPOUND	28
FIGURE 18. TALYSURF CHART SHOWING ELECTRIC DISCHARGE MACHINED MILD-STEEL SURFACE	28
FIGURE 19. OVERALL CONDUCTANCES OF ORDINARY RIGID-SURFACE JOINT AND TYPICAL DIAPHRAGM JOINTS	30

LIST OF TABLES

TABLE 1. MEASURED THERMAL-CONDUCTIVITY VALUES OF CANDIDATE HYDROSTATIC FLUIDS AT ROOM TEMPERATURE	18
TABLE B-1. DIAPHRAGM EFFECTIVENESS VALUES FOR SELECTED VALUES OF JOINT CONDUCTANCE COEFFICIENT	B-4
TABLE B-2. FLUID-POCKET CONDUCTANCE VALUES FOR SELECTED HYDROSTATIC FLUIDS	B-5

ABSTRACT

An experimental program was conducted to evaluate the proof of principle of two new methods for improving thermal conductance of mechanical joints in a vacuum, namely: (1) increasing actual contact surface area at the joint interface by plateauing the microscopic surface asperities, and (2) increasing the joint gross contact area by making one of the mating surfaces a flexible membrane pressurized by a thermally conducting paste or fluid.

Program results showed generally that surface-plateauing methods that employ mechanically induced relative motion with metal-to-metal contact cause galling damage at the surface contact points. Ultrasonic-vibration techniques and pulsed-electric current heating with graphite tools neither damaged the surfaces nor plateaued the asperities.

On the flexible membrane method, analyses indicated that unless a fluid with high thermal conductivity (about an order of magnitude higher than those investigated) can be found, the utility of the flexible-surface diaphragm as a means to increase joint thermal conductance is questionable.

This report describes the experimental program, discusses machined-surface characteristics, thermally conductive fluids, surface plateauing considerations, and flexible-membrane design considerations, and presents the conclusions and recommendations resulting from this investigation.

This research program was initiated in April, 1966, under contract with NASA. This report covers the work performed during the period April 8, 1966, to September 30, 1966.

STUDY TO DETERMINE EXPERIMENTALLY THE
FEASIBILITY OF NEW METHODS FOR IMPROVING
THERMAL CONDUCTANCE OF MECHANICAL JOINTS
IN A VACUUM

by

C. L. Coffin, F. A. Creswick, and J. E. Sorenson

Space missions that call for the vehicle electronic systems to operate at full capacity during orbital residence times of several hours present imposing electronic-package thermal-design problems. If stable and reliable operation of the electronics systems is to be achieved, sufficient heat-transfer paths must be provided to dissipate component heat to the package surroundings. Since orbital flight conditions essentially preclude convective heat transfer from the package external surface, the modes for dissipation are limited to conduction to the supporting structure and radiation to the exposed vehicle internal surfaces. Radiative heat transfer can be influenced by passive control techniques, such as the use of selected surface coatings having the desired emittance. However, the normal variations in environmental temperatures during orbital flight make it undesirable to dissipate electronic-package heat by radiation alone. More positive thermal control is obtained by the use of an active cooling system, whereby each of the electronic packages rejects heat by conduction to a closely controlled constant-temperature heat sink. To be effective, this technique requires low thermal resistance between the electronic packages and their respective heat sinks. It is, therefore, of particular interest to develop a mounting pad that will have low thermal-contact resistance at the mechanical interfaces.

Thermal-contact resistance, which causes a discontinuity in the temperature gradient along the heat path, is a result of physical imperfections and disturbances in the crystal lattice in the material-interface region, which impede the energy-bearing phonons. Consequently, ordinary machined surfaces in contact exhibit an undesirably high thermal resistance at the interface, particularly in a vacuum environment. This resistance can be reduced by a number of methods such as the addition of conductive grease or soft metal foil to the joint. However, all of these methods have certain undesirable features and, so far, no completely satisfactory solution to the problem has been found.

The objective of the proposed research program was to determine experimentally the feasibility of two new methods for improving thermal conductance of mechanical joints which are discussed in the R-ASTR-M Working Paper entitled, "New Method for Thermal Conductance Between Joints in Vacuum", dated January 20, 1965. These methods are

- (1) Increasing actual contact surface area at the joint interface by plateauing microscopic surface asperities with the application of pulsed-heating or the application of ultrasonic vibration
- (2) Increasing the gross contact area by making one surface a flexible membrane backed by hydrostatic pressure from a thermally conducting paste or fluid.

The investigators approached the study on the premise that proof of principle was the main criterion to be used in evaluating the techniques.

This report presents the conclusions and recommendations resulting from the research effort, with attendant discussions of typical machined-surface characteristics, thermally conductive fluids, surface plateauing considerations, and flexible membrane design considerations.

SUMMARY

Consistent with the proof-of-principle evaluation objective of this research program, the main efforts were directed to the experimental investigation of surface-plateauing techniques, the design and construction of a flexible-surface diaphragm (membrane), and the search for suitable thermally conductive hydrostatic fluids or pastes. In addition, the Battelle thermal-conductance measurement apparatus was modified to accommodate cylindrical rigid-to-rigid surface and rigid-to-flexible surface specimen pairs for various axial-loading conditions with a 10^{-4} torr vacuum environment. Supplementary studies were also conducted to classify typical machined surfaces according to roughness and waviness, to assess the possibility of using either conventional or specialized surface-finishing techniques to obtain the desired plateaued-surface effect, and to determine the effectiveness of the flexible-surface diaphragm in conducting heat.

The experiments conducted to identify an effective surface-plateauing technique included (1) frictional heating, (2) electric-current pulse heating, (3) ultrasonic vibration, and (4) fine-grit lapping. Electric-discharge machining also received a cursory examination.

In general the efforts to plateau the microscopic asperities of metallic surfaces were unsuccessful. Attempts to plateau by purely mechanical means when the contacting surfaces were dry resulted in surface galling when relative motion between metallic specimens was induced. This galling damage tended to obscure any beneficial plateauing effects that might have resulted. The application of electric current produced surface pitting with metal-to-metal contact and an apparent slight smoothing with carbon-to-metal contact. Ultrasonic vibration caused localized smoothing on the specimen surfaces, but did not produce the desired plateaued effect.

Several thermally conductive fluids were evaluated in an effort to identify a hydrostatic fluid that would effectively pressurize the flexible-surface diaphragm. The fluids evaluated include the liquid metals mercury, sodium-potassium, and sodium-potassium-rubidium, and slurries consisting of silicone liquids or greases saturated with fine metallic particles of silver, copper, or aluminum powder. The more promising candidate hydrostatic fluids were comparatively evaluated on the basis of measured thermal conductivity.

The search of thermally conductive hydrostatic fluids suitable for diaphragm pressurization did not produce a fluid with the necessary thermal characteristics. All of the fluids examined were found to have relatively low thermal-conductivity values as compared to aluminum. For example, the most promising thermally conductive hydrostatic fluid identified is the liquid-metal sodium potassium (NaK) which has a thermal-conductivity value at room temperature an order of magnitude lower than that of Type 6061 T6 aluminum alloy.

A flexible-surface diaphragm was designed, based on a model of a typical machined surface. However, analysis showed that the presence of even a thin layer of low-conductivity fluid can more than cancel out any beneficial effect that would be derived from flexible-surface conformity. The analysis of diaphragm effectiveness showed that a typical test-specimen diaphragm would be expected to have an effectiveness of only about 7.2 percent. Consequently, the diaphragm could not be expected to compensate for the adverse effect of the low thermal-conductivity hydrostatic fluid.

CONCLUSIONS

It was concluded from the results of this research program that, because of the unavailability of a suitable hydrostatic fluid, the pressurized-diaphragm technique cannot presently be considered promising for increasing joint thermal conductance. In the event that a suitable high-thermal-conductivity fluid can be developed in the future, the flexible-surface conformity approach certainly warrants further consideration.

With regard to surface plateauing, none of the specified methods investigated produced what could be considered to be a plateaued surface, and it is doubtful that surface-processing techniques presently available can be used to effectively plateau metallic surfaces. Even for those techniques that apparently smoothed the surface, the asperities (although reduced in height) did not lose their peaked characteristic. Consequently, it was concluded that regardless of how effectively the candidate plateauing techniques or conventional surface-finishing techniques reduce surface roughness, small surface asperities continue to emerge to maintain the general peak-valley cross-sectional shape. In effect, this points to the condition of small asperities on larger asperities, possibly existing down to sizes approaching the lattice spacing of the crystal-line structure. This, of course, implies that as asperities in a given size range are rounded or flattened, another order of magnification will reveal that the surface is still characterized by peaked asperities.

It is emphasized that although the particular plateauing methods that were investigated in this program did not produce the desired plateaued surface, these experiments did not prove unequivocally that metallic surfaces cannot be effectively plateaued. These experiments did, however, point up a number of problems associated with surface plateauing. In addition to the problem of

surface damage by galling, the problem of work-piece misalignment during the plateauing process is extremely critical. Obviously, when relative motion is induced between mating surfaces, the wear pattern will not be evenly distributed unless the mean lines for the two surface profiles are essentially parallel. The fact that asperity heights characterizing the types of surfaces considered in this study are microscopic requires that allowable tolerance for misalignment of the mating surfaces normal to their common centerline be also essentially microscopic.

It is noted that because the tendency of a given plateauing technique is to reduce surface roughness, initially smooth surfaces provide the best surfaces for evaluating plateauing techniques; this was confirmed by experimental program results.

It was further concluded that of the plateauing methods investigated, only the ultrasonic-vibration and the pressed-carbon-tool pulsed-current methods are worthy of further consideration. As previously noted, the other methods produced badly damaged surfaces.

RECOMMENDATIONS

If further research is carried out on methods of increasing joint conductance, it is recommended that the work be directed initially to the identification and/or development of a high-thermal-conductivity hydrostatic fluid or paste.

With regard to surface-plateauing methods, it is recommended that any further efforts deal primarily with the development of surface-finishing methods (machine, chemical, or electro-chemical) that will deform the lowest order of surface asperities that can be identified.

EXPERIMENTAL PROCEDURES

Measurements of hydrostatic fluid thermal conductivities and experiments to assess the effectiveness of various rigid-surface plateauing techniques were carried out in the Battelle Mechanical Engineering Laboratory. Much of the experimental equipment used for these investigations was specially designed for this program and fabricated in the Laboratory; the test specimens were made in the Battelle machine shop.

Although the preliminary experimental findings precluded the need for joint thermal-conductance measurements, Analytical Physics Division personnel completed the modification of the Battelle conductance-measuring apparatus to

accommodate test specimen pairs under various axial-load conditions in a vacuum environment with pressures less than 10^{-4} torr.

Test-Specimen Design Considerations

Specimen-Material Selection

Type 6061-T6 aluminum alloy was used to fabricate both the flexible-surface diaphragm specimens and the rigid-surface plateauing specimens used during this study.

It was determined through investigation of surface friction phenomena that asperity deformation is influenced to a higher degree by the material melting temperature than by the material hardness. This in turn indicated that a metal with a relatively low melting point, such as aluminum (660 C) will require less energy to effect the same degree of asperity deformation than will higher melting point metals. Consequently, considering both the low melting point and the relative ease of fabrication for aluminum alloy, Type 6061-T6 aluminum was selected for the plateauing-investigation specimens.

Type 6061-T6 aluminum alloy was also attractive as the diaphragm material because of its low elastic modulus and the attendant characteristic of allowing good conformability to the rigid surface.

Rigid-Surface Specimen Design

A total of 34 Type 6061-T6 aluminum cylindrical specimens, 1 inch in diameter by 5 inches long, were fabricated preparatory to the rigid-surface plateauing technique investigation. These specimens were machined to have end-surface finishes of 8 microinches, 63 microinches, 125 microinches, and 500 microinches centerline average (CLA). This wide variation was selected as a means of assessing the type of surface most amenable to plateauing. All of the test surfaces were machined with concentric surface lay to provide symmetry.

Surface-Plateauing Procedures

The prescribed rigid-surface plateauing investigation consisted of a series of preliminary experiments involving frictional heating, ultrasonic vibration, and pulsed electric current heating with specimen pairs having various surface finishes. If the result of a given preliminary plateauing test was judged to be promising on the basis of a change with no apparent damage, the specimen surfaces were further analyzed with the Talysurf surface-roughness analyzer. However, if surface damage occurred, the plateauing technique responsible for the damage was eliminated from

further consideration. For each technique examined, when appropriate, parameters such as contact pressure and relative surface speed were varied and several individual tests were conducted.

Mechanical-Friction Plateauing Methods

Figure 1 is a photograph showing the device that was used to impart translatory motion to the rigid-surface specimens for the plateauing experiments, and Figure 2 shows a specimen pair set up on a drill press for testing. Rotary relative motion was provided by the drill press.

The translatory motion device was powered by a 1/2-horsepower drill motor with a maximum frequency of about 1.7 cycles per second. Drill motor speed, and, therefore, the frequency of the translatory motion, could be varied through adjustment of an a-c brush-motor speed control placed in series with the drill motor. Rotational speed could be varied from about 350 to 2280 rpm by changing belt pulleys on the drill press. It was found initially that the low speed, 350 rpm, was the most convenient for these plateauing tests.

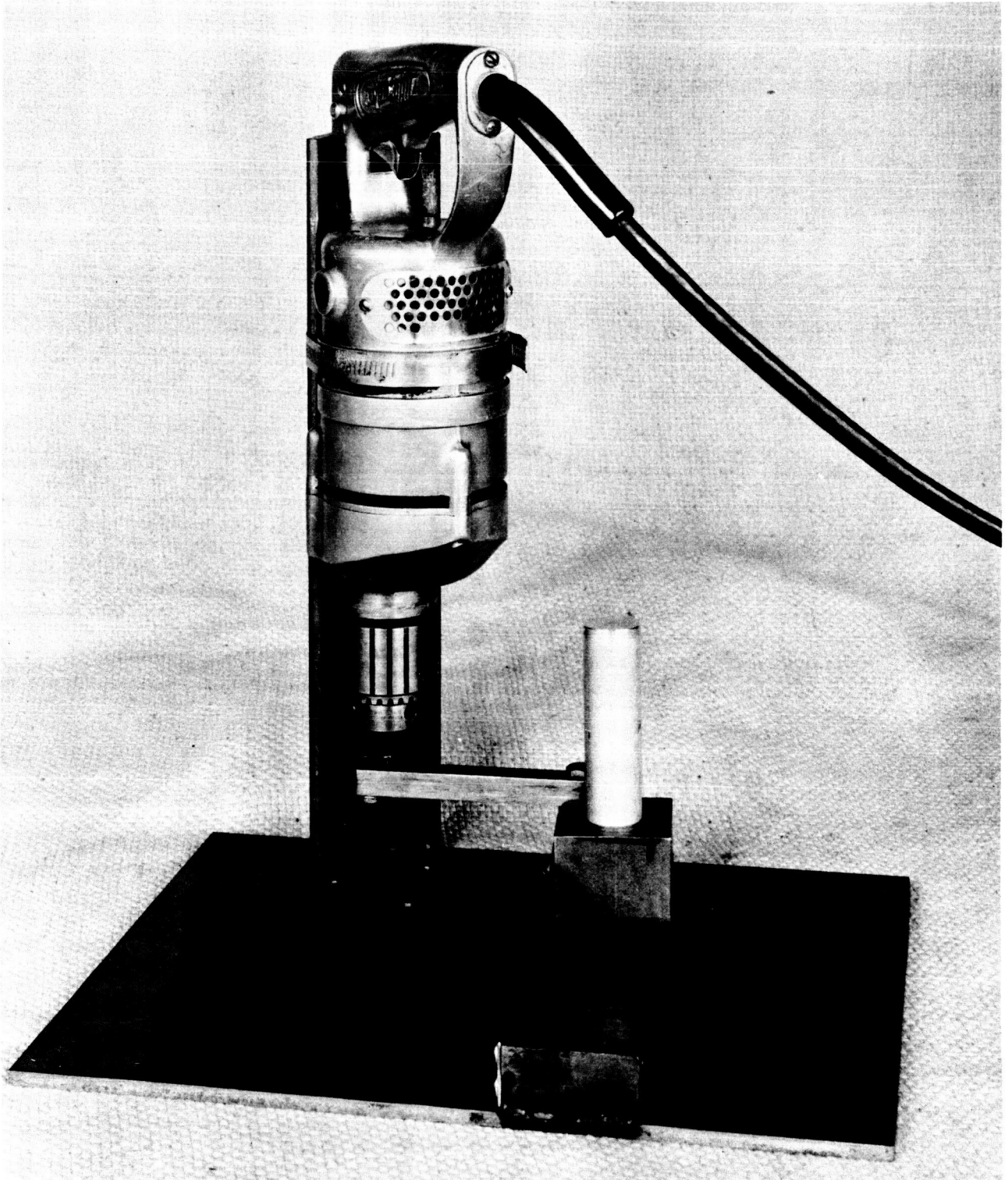
To perform a test, the specimen surfaces were brought into contact by lowering the revolving upper specimen until it contacted the bottom oscillating specimen. For a given test if galling did not occur upon contact, contact pressure was increased gradually until a noticeable surface change was observed. The surface characteristics, particularly the lay pattern, of the specimens that were used permitted visual assessment of surface change with little or no magnification. For those tests which resulted in surface galling, the galling occurred almost at the instant of contact with the application of almost negligible pressure.

Ultrasonic-Vibration Methods

Ultrasonic-vibration plateauing experiments were conducted using transducers to provide both axial and transverse relative motions.

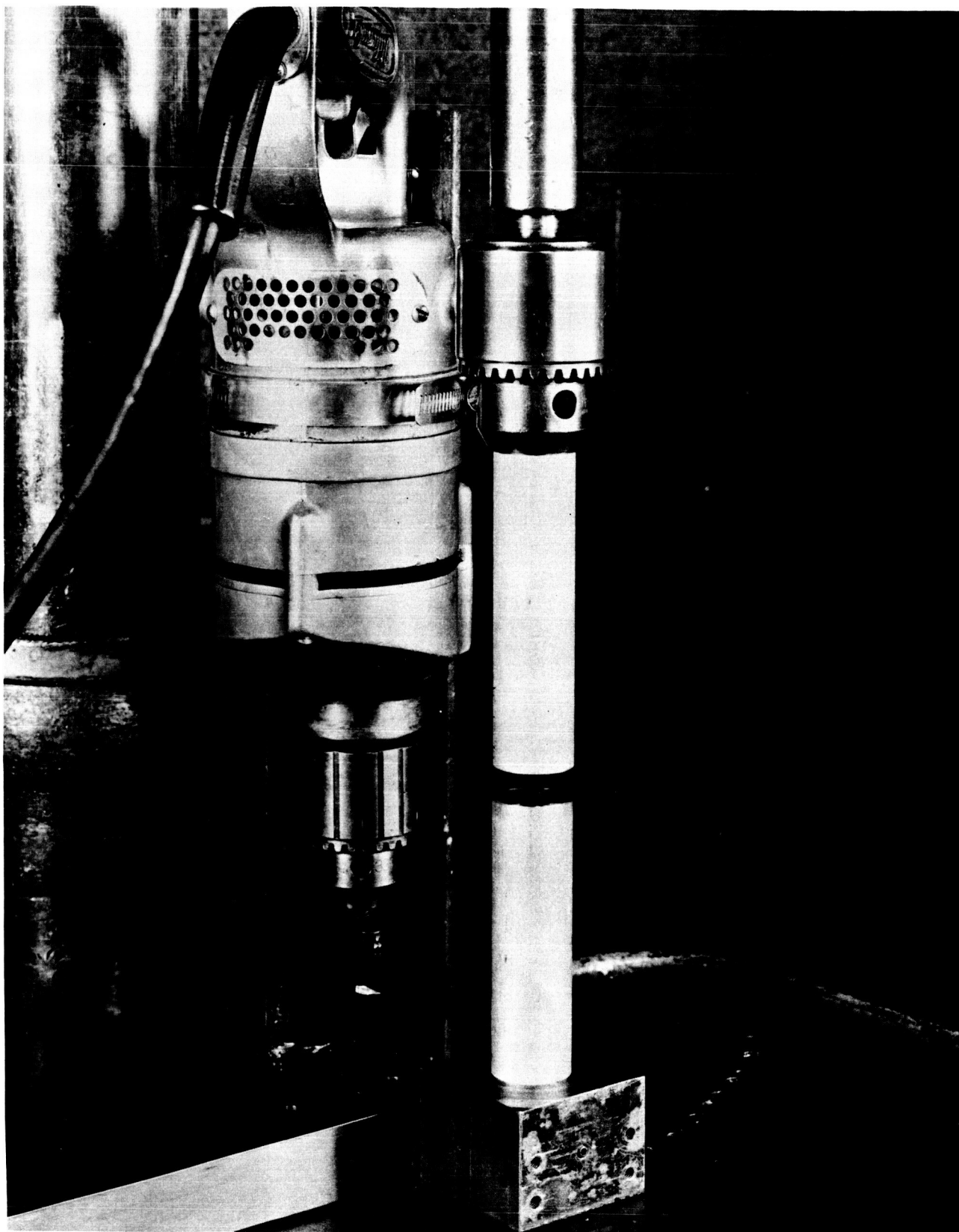
As shown in Figure 3, axial relative-motion (high-frequency peening) tests were carried out using a lathe to provide rotary motion in conjunction with an ultrasonic transducer head to generate the longitudinal vibration in the test specimen. For these tests the vibrating specimen had a frequency of about 20 kilocycles and the lathe-driven specimen had a nominal rotational speed of 250 rpm. The power supplied to vibrate the specimen was varied from about 100 to 500 watts.

Figure 4 shows the laboratory setup that was used for the ultrasonic-vibration translatory relative motion tests. The transducer head, as shown, vibrated a stainless steel tool laterally at a frequency of about 20 kilocycles. Power supplied to vibrate the specimen was varied from about 100 to 500 watts. For the setup as shown, contact pressure between the tool and the test specimen was manually applied through a lever arrangement that effected an axial load.



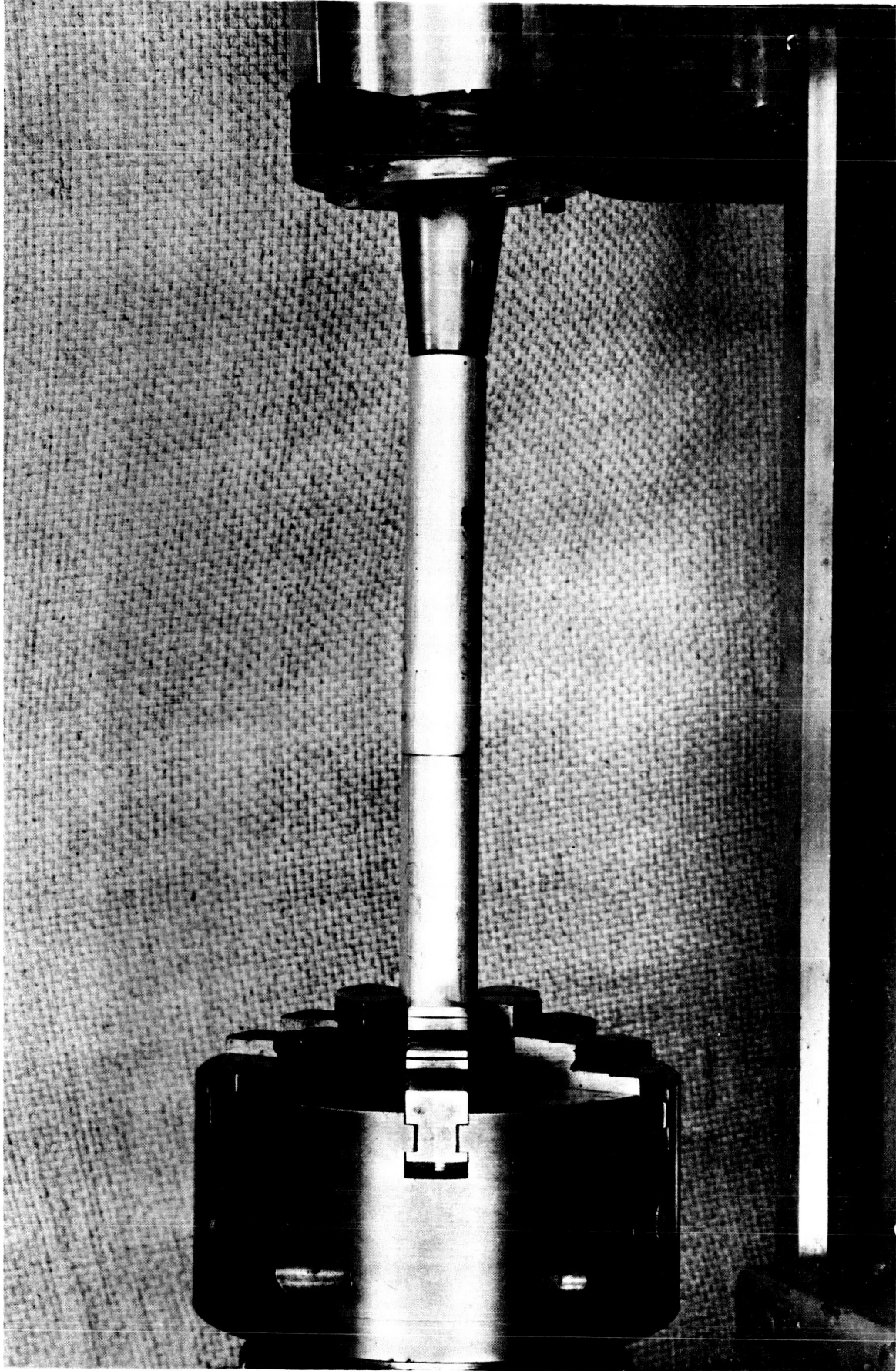
35569

FIGURE 1. DEVICE USED TO IMPART TRANSLATORY RELATIVE MOTION TO RIGID SURFACES FOR THE PLATEAUIING STUDIES



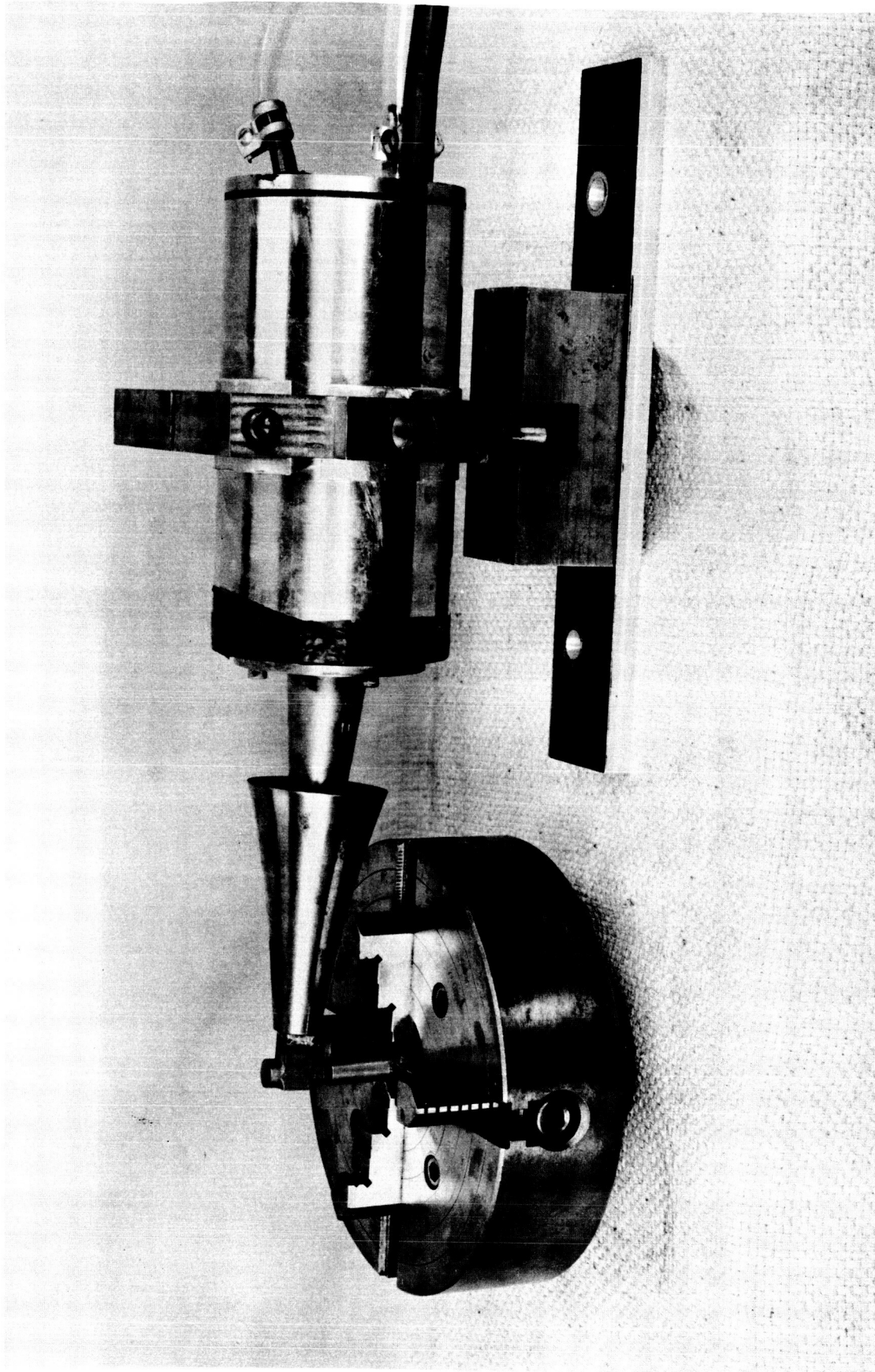
35568

FIGURE 2. RIGID-SURFACE SPECIMEN-PAIR SETUP FOR AN EXPERIMENT



35567

FIGURE 3. LATHE SETUP WITH ULTRASONIC TRANSDUCER USED FOR AXIAL-RELATIVE-MOTION ULTRASONIC-VIBRATION TESTS



35570

FIGURE 4. FIXTURE SETUP WITH ULTRASONIC TRANSDUCER USED FOR TRANSLATORY RELATIVE MOTION ULTRASONIC-VIBRATION TESTS

Electric-Heating Methods

The electric-current-pulse plateauing tests were conducted with essentially the same relative motion as the frictional-heating tests and with the addition of electric heating. Relative translatory and rotary motions were obtained by using the test setup shown in Figure 2. In addition, the rotating specimen was fitted with brushes to conduct the electric current.

For these tests the specimen pairs served as conductors in series with a 250-ampere-maximum d-c welder. A constant voltage of about 40 volts across the specimen pair was used to provide the necessary current to the specimens for each of the tests. The magnitude of the current pulses was increased from test to test until a surface change could be detected. For those tests involving surfaces that tended to gall, the current was applied at almost the instant of contact in an attempt to produce a result that could be attributed primarily to the effect of electric-current (I^2R) heating. This galling problem precluded the sustained application of pulsed current with metal-to-metal contact. However, sustained current application was accomplished by using a pressed carbon tool as the rotating plateauing specimen.

Hydrostatic Fluid Thermal-Conductivity Measurement

A simple, electrically heated, annulus-type thermal-conductance measurement rig fabricated in the laboratory was used to evaluate the thermal conductivity at room temperature of candidate hydrostatic fluids.

Figure 5 is a schematic diagram of the conductance-measurement device that was used. As shown, the fluid or paste material to be evaluated was placed in the annulus between the electric-resistance heater and the outer container. The power supplied to the heater was adjusted at regular intervals until a steady-state condition was established. With the steady-state condition prevailing, temperatures across the test fluid were recorded with thermocouples, and the fluid thermal conductivity was then calculated from the following equation for conduction across an annulus, from Reference (1):

$$k = q' \frac{\ln(r_2/r_1)}{2\pi(T_1 - T_2)} \cdot \quad (1)$$

Although the primary interest was in how the conductivity values for the various fluids compared to each other and to 6061-T6 aluminum alloy, a simple error analysis was performed by measuring the thermal conductivity of a silicone fluid of known value to assess the magnitude of experimental deviation. For the fluids used for the error analysis, measured values agreed with the manufacturer's published values within 5 percent.

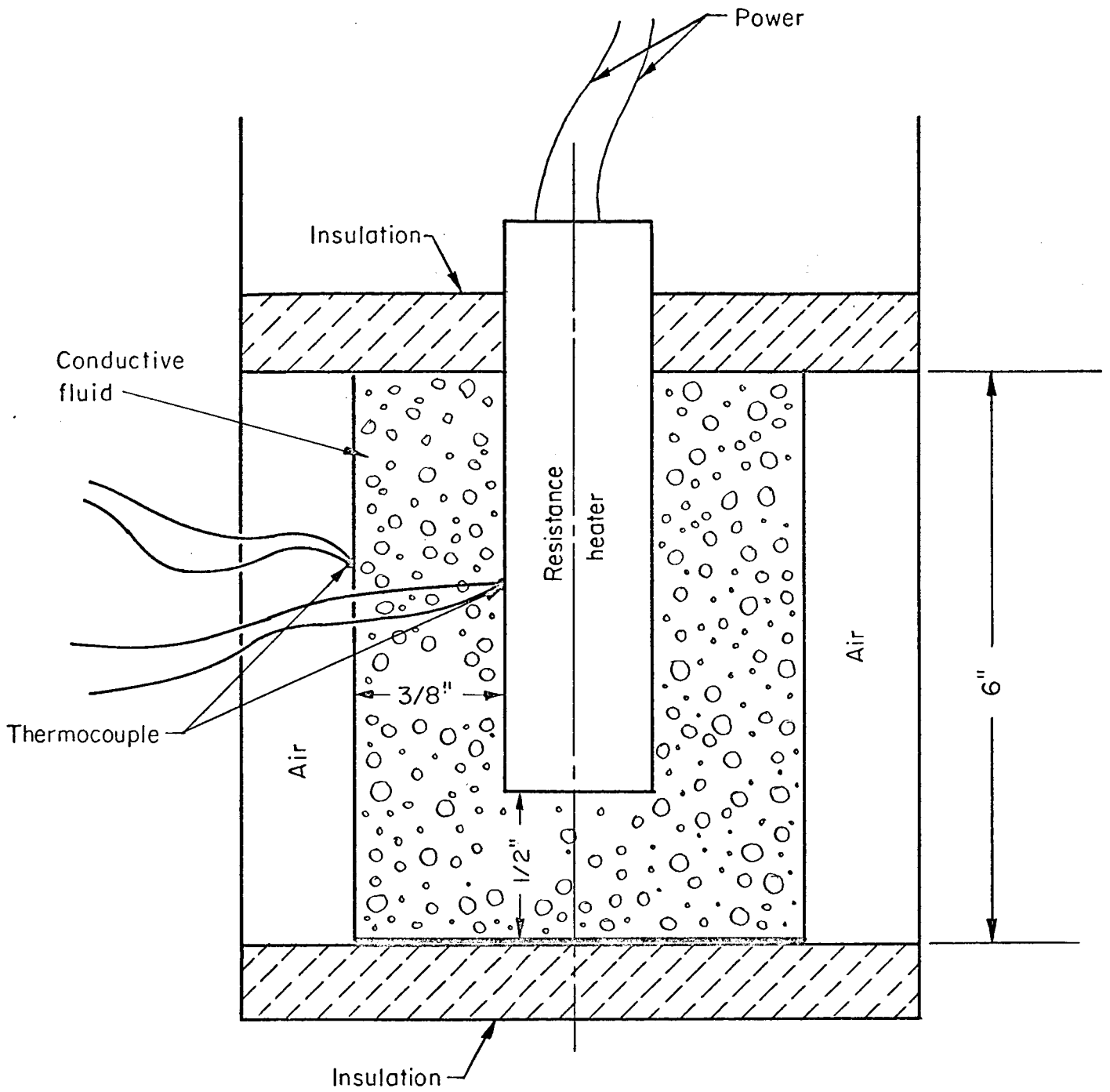


FIGURE 5. APPARATUS FOR MEASURING HYDROSTATIC FLUID THERMAL CONDUCTIVITY

Machined-Surface Characteristics

Preparatory to the design of the diaphragm and rigid-surface specimens, literature pertaining to metallic-surface characteristics and to contiguous-surfaces phenomena was surveyed in an effort to obtain the information needed to establish a relationship between surface roughness and surface waviness that would serve as a guide for specifying surface finish and diaphragm thickness. The primary emphasis was directed to the classification of typical machined surfaces according to roughness, waviness, lay, and asperity geometry. Statistical data providing roughness and waviness amplitude as a function of wavelength for various machined surfaces was the type of surface microtopography information sought. These statistical data were not found and may not yet be available; however, sufficient data relative to specific surfaces were available for use in the design of the diaphragm and rigid-surface specimens.

The literature indicates that for the types of machined surfaces considered for this study, waviness assumes essentially a periodic form with wavelength exceeding amplitude by a significant amount. Also, asperity height is generally less than the waviness amplitude, even for comparatively rough surface finishes. It is additionally noted that asperity profile, for a given surface, depends to a large extent on the direction of the lay. This is, in effect, the influence of the finishing marks that establish surface lay condition consistent with the material surface structure.

As noted in Reference (2), conventional machining techniques produce waviness wavelengths in the order of from 0.040 to 1.0 inch with amplitudes (peak-to-valley displacement) ranging from approximately 1×10^{-6} to 5×10^{-4} inch. [Battelle staff members concerned with the development of new and refined surface-finishing techniques indicate that recent advances have made it possible to achieve virtually zero surface waviness with attendant roughness in the order of 1 micro-inch for relatively hard materials by conventional surface-finishing processes such as machine lapping and superfinishing. The superfinishing process is described in References (3) and (4)].

FLEXIBLE-SURFACE DIAPHRAGM DESIGN

In order to design a diaphragm that will readily adapt itself to the shape of the mating surface, three important parameters must be considered. These are the pressure acting on the diaphragm, the wavelength of the surface waviness, and the amplitude. In addition, because it does not appear possible to design a diaphragm to withstand the required pressures without being in contact with the mating surface and yet be flexible enough to conform to the mating surface, means must be provided whereby the pressure can be applied after the joint is assembled. Another possibility is to design the diaphragm with a slight

outward bulge so that as the joint is assembled and the diaphragm forced to conform to the mating surface the slight decrease in volume in the enclosed space behind the diaphragm is enough to create the required pressures (it is assumed that the thermally conductive paste is essentially incompressible).

Figure 6 shows the influence of the wavelength (λ) and the amplitude (δ) of the surface waviness on the diaphragm design. The diaphragm should be flexible enough so that under the action of the pressure (P) it will conform to the mating surface as shown in Figure 6b.

As previously noted, conventional surface-machining practices can be expected to produce waviness wavelengths in the order of 0.40 to 1.0 inch with amplitudes ranging from approximately 1×10^{-6} to 5×10^{-4} inch. For the preliminary design of the flexible-surface-specimen diaphragm, a wavelength of 0.30 inch with an amplitude of 0.0007 inch were selected as typical midrange values that could be obtained easily by standard machining practice. Figure 7 is a schematic of an example of the model surface profile used for the diaphragm design.

The following expression is derived in Appendix A for the diaphragm thickness required to obtain complete contact with a rigid surface with unidirectional lay:

$$t = \left[\frac{P\lambda^4}{65ES} \right]^{1/3} \quad (2)$$

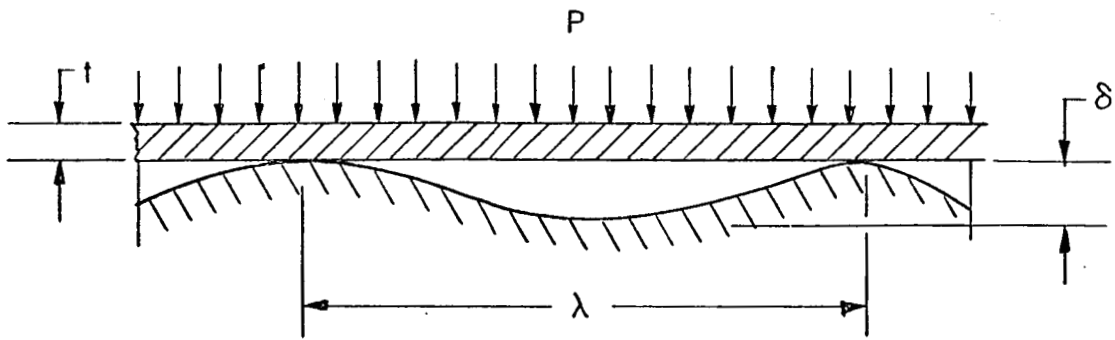
Evaluating this expression using the model surface-waviness characteristics, the mechanical properties of Type 6061 aluminum and fluid pressure of 1000 psia resulted in a thickness of 0.026 inch. (The value for fluid pressure was arrived at by assuming the total load supported by the diaphragm was equal to the working tensile load of a 1/4-inch stainless steel cap screw.)

The resulting value for diaphragm thickness was judged to be satisfactory in that it was in the range of commercially available thicknesses and would not present any extreme problems in being welded to the supporting rim structure.

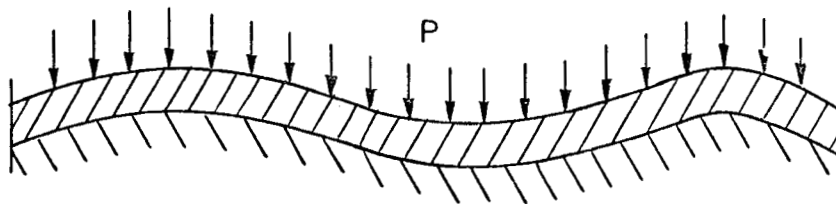
DISCUSSION OF PROGRAM RESULTS

Search for Thermally Conductive Fluids

In the investigation of conductive hydrostatic fluids, a number of candidate fluids were experimentally evaluated in an effort to find an effective means for using pressurized flexible-membrane surfaces. A comparative evaluation was made on the basis of thermal-conductivity values determined by a steady-state



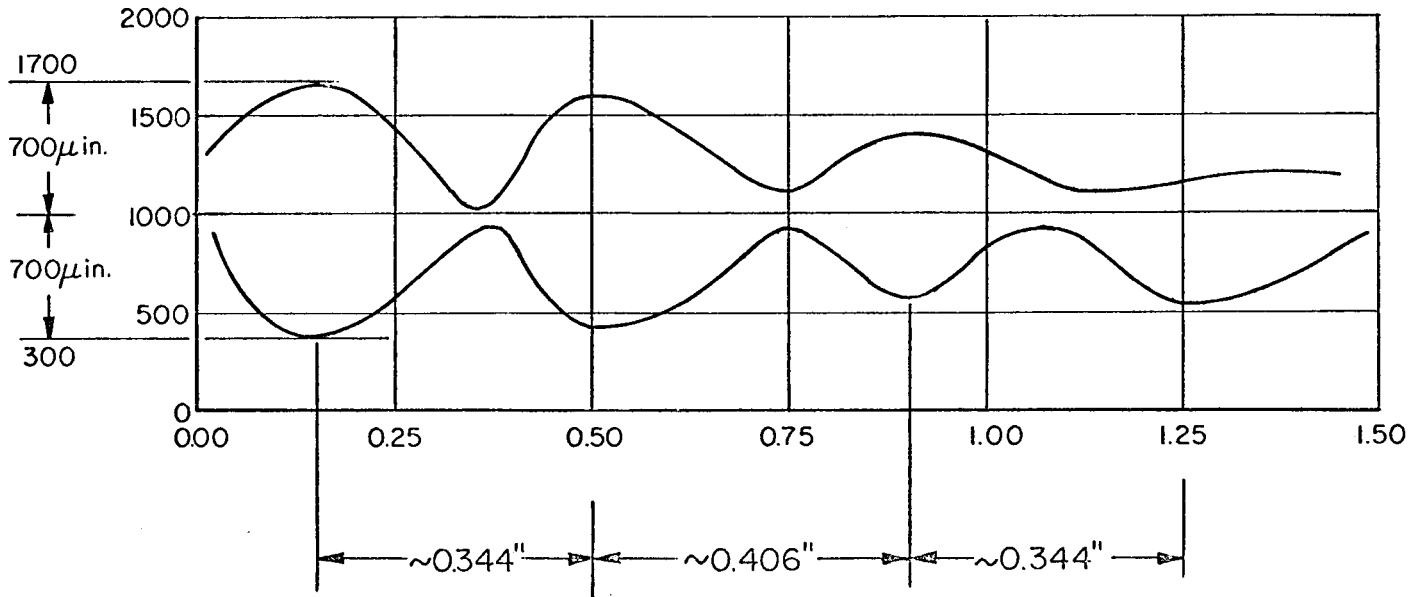
a) Diaphragm in Contact with Mating Surface



b) Diaphragm Conforming to Shape of Mating Surface

FIGURE 6. SCHEMATIC DIAGRAM OF FLEXIBLE SURFACE DIAPHRAGM AND MATING SURFACE

Reference (5)



Amplitude $\sim 700 \times 10^{-6}$ in. = 0.0007 in.
Wavelength ~ 0.375 in.

FIGURE 7. TYPICAL SURFACE WAVINESS PROFILE USED FOR THE FLEXIBLE SURFACE DIAPHRAGM DESIGN

heated-annulus technique described in the Experimental Procedures section of this report. Methods used initially to identify potential hydrostatic fluids included a review of the pertinent literature, discussions with vendors and Battelle staff members, and formulations that intuitively appeared attractive.

Silicone-Fluid/Metal-Particle Slurries

At the outset of the search for thermally conductive fluids, it was felt that a slurry or paste of metallic particles in silicone fluid or grease might be attractive, the silicones being chemically inert and physically stable at normal temperatures and the metallic particles providing a good conductive heat path.

The requirement that the hydrostatic fluid used for diaphragm pressurization have a consistency that would permit convenient specimen loading and at the same time provide a uniform pressure within the diaphragm cavity essentially limited the amount of metallic powder that could be added to a given quantity of silicone fluid or grease. Consequently, the mixtures selected for evaluation represented a compromise between metallic particle content and fluidity. Low-viscosity silicone fluids, in general, accommodated a higher percentage of metallic powder than the silicone greases for a given degree of fluidity.

Table 1 presents representative results from the silicone-fluid/metallic-particle conductivity-measurement tests. These results show that although the presence of metallic powders in the silicone fluids and greases serves to increase the thermal conductivity regardless of the quantity of metallic powder used, the conductivity value for the mixture is extremely small compared to that for Type 6061 aluminum alloy. Test results and the simple thermal-model calculations indicated that the maximum thermal-conductivity value to be expected from a silicone-fluid/metal-particle paste is in the order of 1.5 to 2 Btu/hr-ft-F.

To check this experimental result, a brief analytical study was undertaken. Considering that the thermal conductivity of the silicone fluids that were considered in this study is on the order of 0.09 Btu/hr-ft-F, it is obvious that if the conducting fluid is to have a conductivity value approaching anywhere near that of aluminum, the metallic powder must have a substantial effect on the conductivity of the paste. Results of calculations, based on an extrapolation of experimental results with a simple thermal model, indicated that a paste containing only 5 percent silicone fluid will still have only about 1/50th the conductivity of the metal powder alone.

Liquid Metals

In view of the poor conductivities exhibited by the silicone-fluid/metallic-powder slurries, sodium-potassium and mercury liquid metals were evaluated as possible alternates. The use of liquid metals had originally been considered questionable for design application on the basis of the damage that might occur in the event of a rupture of the flexible diaphragm, particularly in a zero-g environment. In an effort to overcome this problem, mercury

TABLE 1. MEASURED THERMAL-CONDUCTIVITY VALUES OF CANDIDATE
HYDROSTATIC FLUIDS AT ROOM TEMPERATURE

Conductive Material	Thermal Conductivity, Btu/hr-ft-F
Copper powder in silicone grease, copper - 39.8 percent by weight	0.16
Copper powder in silicone grease, copper - 75.9 percent by weight	0.43
Copper powder in Dow-Corning No. 200 silicone fluid (viscosity 100 cs at 25 C), copper - 76.8 percent by weight	0.4
Dow-Corning No. 200 silicone fluid (no filler)	0.1
Aluminum powder in silicone grease, aluminum - 39.7 percent by weight	0.2
Silicone grease (no filler)	0.092
Copper powder, slightly compacted	0.1
Type 6061 T6 aluminum alloy	115

was combined with silver powder to form an amalgam paste containing approximately 91.8 percent mercury by weight. It was theorized that paste-like consistency of such an amalgam would permit the material to stay agglomerated in the event of a diaphragm rupture in a vacuum environment. Silver filler, in addition to its relatively high thermal conductivity, exhibits a very good surface wettability for mercury.

It is probable that the thermal conductivity of this amalgam would be at least as good as that for pure mercury, which is 5 Btu/hr-ft-F. However, it was desired that a higher conductivity fluid be used in the laboratory to show proof of principle for the diaphragm pressurization technique. Consequently, NaK was tentatively selected on the basis that it has the highest thermal conductivity of all room-temperature liquids, about 15 Btu/hr-ft-F at room temperature. However, it is noted that this value is quite low when compared to the value for Type 6061 T6 aluminum alloy, which is about 115 Btu/hr-ft-F. The aluminum value is approximately an order of magnitude greater than the NaK value.

General Considerations

Thermal-conductivity values for a given substance depend, of course, on the chemical composition, the physical structure, and the material state. The lowest thermal-conductivity values occurring in nature are associated with inorganic and organic gases and vapors, whereas the highest values are for pure, crystalline metallic materials, with values for liquids and amorphous substances such as greases somewhere in between. Current theory indicates that heat transmission in liquids results from oscillatory longitudinal vibrations somewhat analogous to the mechanism of sound propagation. Since this oscillatory transport of energy is restricted by the irregular arrangement of the molecules and atoms, liquid thermal-conductivity values are characteristically low compared to those of metals. For example, water, the best conductor of all nonmetallic liquids, has a thermal-conductivity value of approximately 0.4 Btu/hr-ft-F, or about 1/350th of that for Type 6061 aluminum at the same temperature.

An order-of-magnitude study showed that even NaK does not have a high enough thermal conductivity to make the pressurized-diaphragm concept attractive. This point is discussed further in the section on Diaphragm Effectiveness.

Since this is the case, it is clear that any further investigation of this concept should be aimed primarily at the search for a better fluid. It cannot be stated that an acceptable fluid does not exist; however, the likelihood appears remote.

Plateauing Investigation

Mechanical Plateauing

The literature pertaining to metallic surface characteristics and surface contact phenomena describes, in detail, how asperity tips are affected when

two surfaces are brought into contact under load, the result being plastic deformation with work hardening. The literature also tells us that for a typical asperity distribution the load required to promote tip deformation up to the point of plastic flow is quite small. For example, Reference (6) indicates that loads of less than 0.1 gram normal to the surface will initiate full plasticity in the longest surface asperities of tool steel. This implies that when metal surfaces are in contact with even small loads, the material which forms the finer surface asperities is subjected to stress levels in excess of its elastic limit. From this it was considered probable that the degree of asperity deformation sought in this program could be accomplished by localized heating at the specimen-pair joint interface. Consequently, experiments were conducted to determine if the frictional heating generated by relative motion during the plateauing process was sufficient to cause the desired gross-asperity deformation with little or no external heating.

The characteristics and results of the preliminary friction-heating plateauing experiments are listed below. In each case, frictional heating was induced by moving the contacting surfaces relative to each other by the method described in the Experimental Procedures section. This technique essentially incorporates rotary and translatory relative motions induced mechanically, in conjunction with a light contact pressure from a manually applied axial load.

Aluminum Against Aluminum, Surfaces Dry. As shown in the photograph in Figure 8, this technique caused severe galling which damaged the contacting surfaces.

Aluminum Against Aluminum, Surfaces Lubricated With Kerosine. No galling initially, but the lubrication film eventually ruptured, and the resulting galling damaged the contacting surfaces. Figure 9 is a photograph of the test surfaces.

Aluminum Against Aluminum, Surfaces Lubricated With Light Machine Oil. There was no apparent effect because the oil film served to lubricate the surfaces and prevent effective contact.

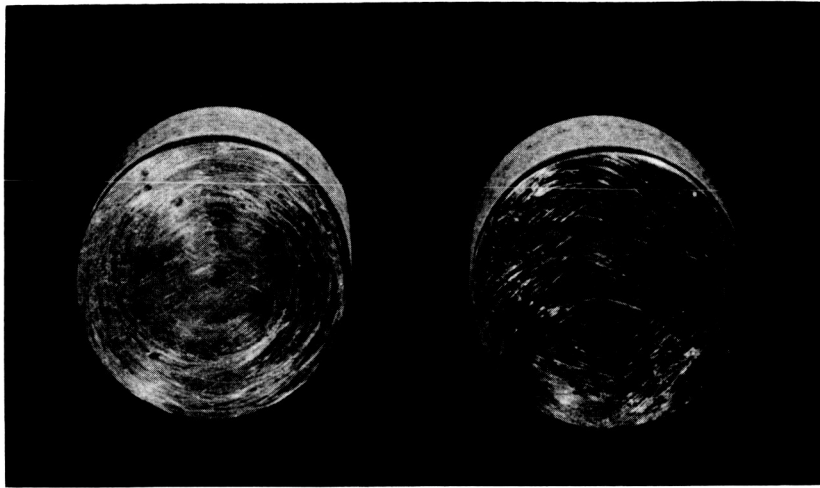
Aluminum Against Stainless Steel, Surfaces Dry. As shown in the photograph in Figure 10, the result was a light galling which produced a somewhat spotty surface.

Aluminum Against Stainless Steel, Surfaces Lubricated With Kerosine. No galling, but the lubrication film eventually ruptured and the resulting galling damaged the contacting surfaces. The test surfaces are shown in the photograph in Figure 11.

Aluminum Against Pressed Graphite Surfaces Dry. There was no apparent effect.

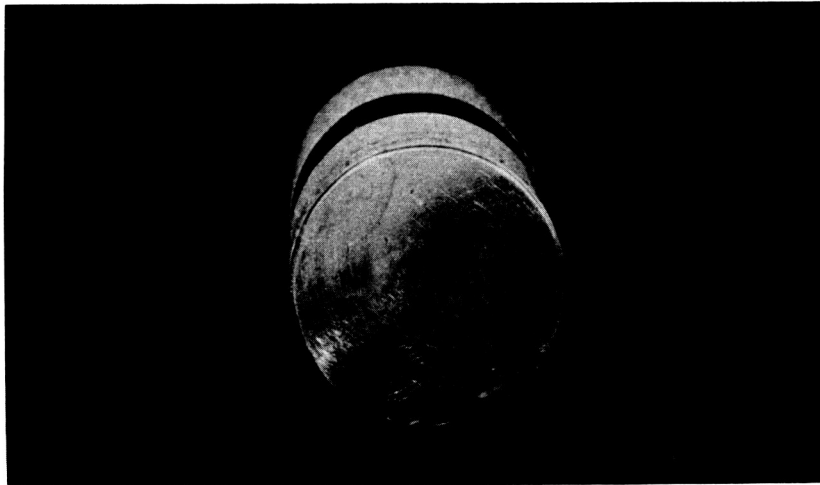
Ultrasonic-Vibration Plateauing

Ultrasonic-vibration techniques were also investigated as potential methods of plateauing metallic surfaces by the generation of localized frictional



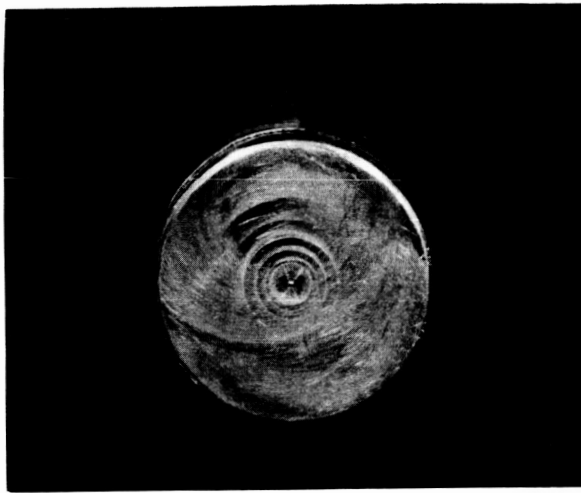
35561

FIGURE 8. SEVERE GALLING DAMAGE OF ALUMINUM SURFACES CAUSED BY RELATIVE MOTION WITH SPECIMEN SURFACES DRY



35562

FIGURE 9. SEVERE GALLING DAMAGE OF ALUMINUM SURFACES CAUSED BY RELATIVE MOTION WITH SPECIMEN SURFACES LUBRICATED WITH KEROSENE



35563

FIGURE 10. LIGHT GALLING DAMAGE OF ALUMINUM AND STAINLESS STEEL CAUSED BY RELATIVE MOTION WITH SPECIMEN SURFACES DRY



35564

FIGURE 11. LIGHT GALLING DAMAGE OF ALUMINUM AND STAINLESS STEEL SURFACES CAUSED BY RELATIVE MOTION WITH SPECIMEN SURFACES LUBRICATED WITH KEROSENE

heating with very small relative displacements. The ultrasonic experiments included tests in which the surfaces were vibrated relative to each other longitudinally and tests where the contacting surfaces were vibrated with a translatory shearing motion. The ultrasonic-vibration plateauing methods used in this investigation are discussed in detail in the Experimental Procedures section.

In general, ultrasonic vibration produced a localized smoothing effect, but the resulting surface changes characterized grinding rather than plateauing.

The preliminary ultrasonic-vibration plateauing tests conducted are listed below. The 1-inch-diameter aluminum specimens were found to be ineffective for the shearing tests, apparently because of the relatively high rate of heat conduction away from the vibrating surfaces.

Aluminum Against Aluminum, Surfaces Dry. A rotary motion was induced mechanically, an axial motion (high-frequency peening) was induced by ultrasonic vibration, and a light contact pressure was produced by manually applied axial load. Result: This technique resulted in light surface galling that produced a spotty surface.

Mild Steel Against Stainless Steel, Surfaces Dry. A translatory motion was induced by an ultrasonic vibration and a light contact pressure was maintained by a manually applied axial load. Result: As shown by the Talysurf chart in Figure 12, the specimen surface was apparently smoothed locally at the contact points, but the asperities were not plateaued.

Stainless Steel Against Stainless Steel. A translatory motion was induced by ultrasonic vibration and a light contact pressure was maintained by a manually applied axial load. Result: As shown by the Talysurf chart in Figure 13 the high point on the test-specimen surface was apparently smoothed by the shearing action of the tool, but the asperities were not plateaued.

Pulsed Heating

The electric-current-pulse-heating surface-plateauing experiments were performed essentially the same as the frictional-heating experiments but with heat augmentation (I^2R). For the tests listed below, rotary and translatory relative motions were induced mechanically, a light contact pressure was provided by a manually applied axial load, and electric current was applied up to 200 amperes at 40 volts.

The application of electric current produced localized arcing with attendant surface pitting with metal-to-metal contact, and an apparent slight smoothing effect with carbon-to-metal contact. All of the metal-to-metal contact experiments were conducted with the surfaces dry, and in each case surface galling either preceded or accompanied the pitting.

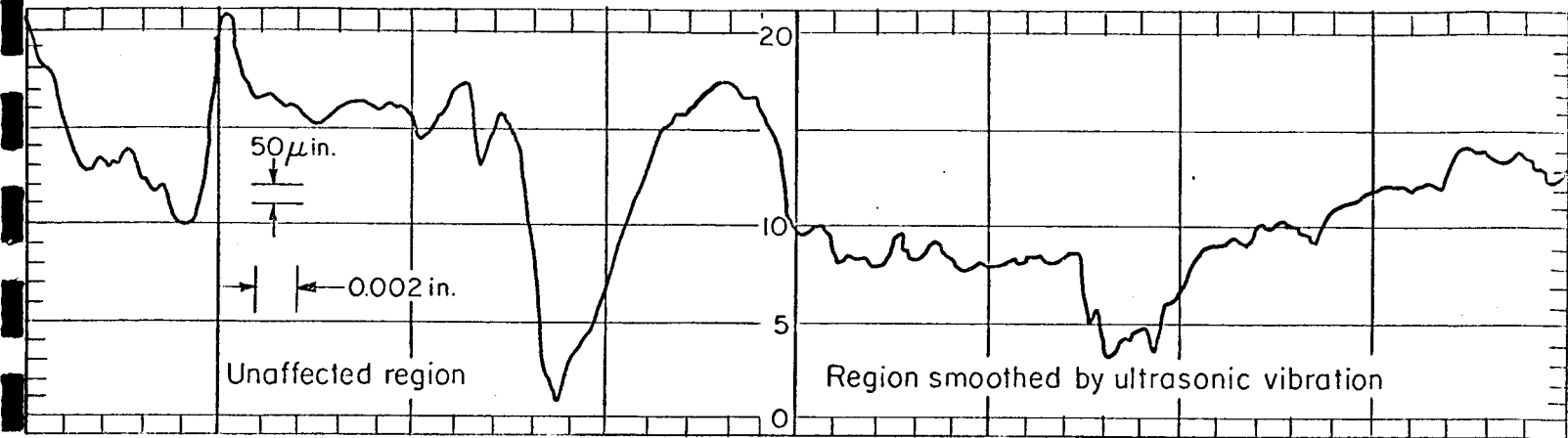


FIGURE 12. TALYSURF CHART SHOWING APPARENT SMOOTHING EFFECT OF ULTRASONIC VIBRATION IN A REGION OF A MILD STEEL SURFACE

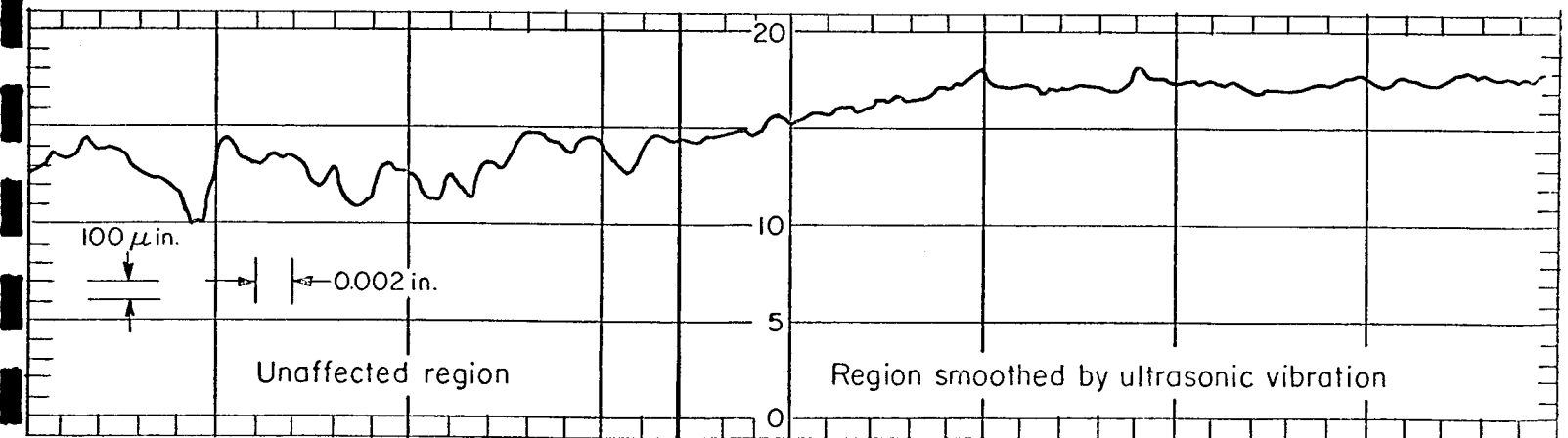


FIGURE 13. TALYSURF CHART SHOWING APPARENT SMOOTHING EFFECT IN A REGION OF A STAINLESS STEEL SURFACE

Aluminum Against Aluminum, Surfaces Dry. As shown by the photograph in Figure 14 this approach produced badly pitted and galled surfaces.

Aluminum Against Stainless Steel, Surfaces Dry. As shown by the photograph in Figure 15 this method also produced badly pitted and galled surfaces.

Aluminum Against Pressed Graphite, Surfaces Dry. As shown by the Talysurf chart in Figure 16 this technique caused an apparent slight smoothing of the specimen surface (similar to grinding), but the asperities were not plateaued.

Lapped Surface

Preliminary results of the plateauing investigation indicated that, as a surface is smoothed by the shearing action of relative motion with another surface, asperity height is generally reduced but asperity profile tends to remain essentially peaked. In an effort to determine if the mechanism of surface metal flow would flatten or round-off asperity peaks, the surface of one of the aluminum specimens was lapped to a nominal roughness of 3.1 microinches CLA. This lapped surface served as the ultimate standard for the aluminum surface plateauing investigation. As shown in the Talysurf chart in Figure 17, even with this relatively smooth surface the asperities retained their general peaked characteristic.

Electric Discharge Machining

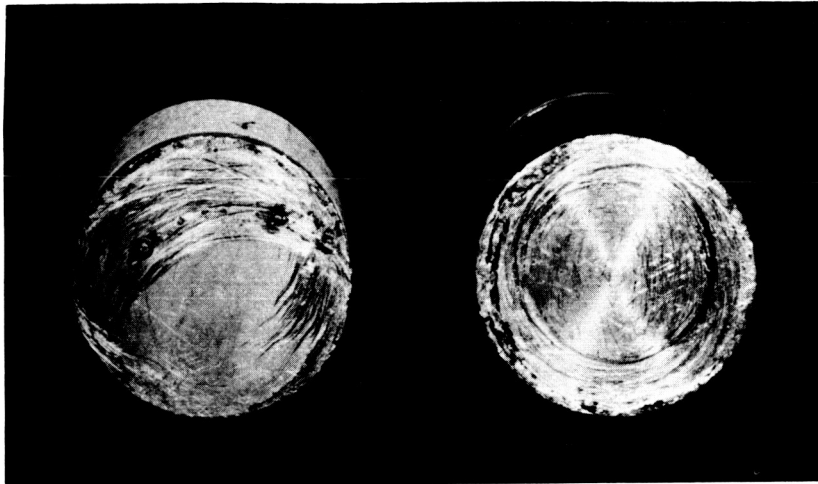
During the investigation of available metallic-surface-finishing methods, cursory visual observations of metal surfaces prepared by electric-discharge-machining techniques (EDM) indicated that these surfaces exhibit the desired plateaued asperity characteristics. However, as shown in the Talysurf chart in Figure 18, the asperities on the sample surface prepared by EDM retain their peaked characteristic. Consequently, electric discharge machining does not appear to be an effective means of plateauing surface asperities.

General Considerations

In conducting and evaluating the results of the plateauing studies, some basic effects in trying to achieve the desired surface finish were observed.

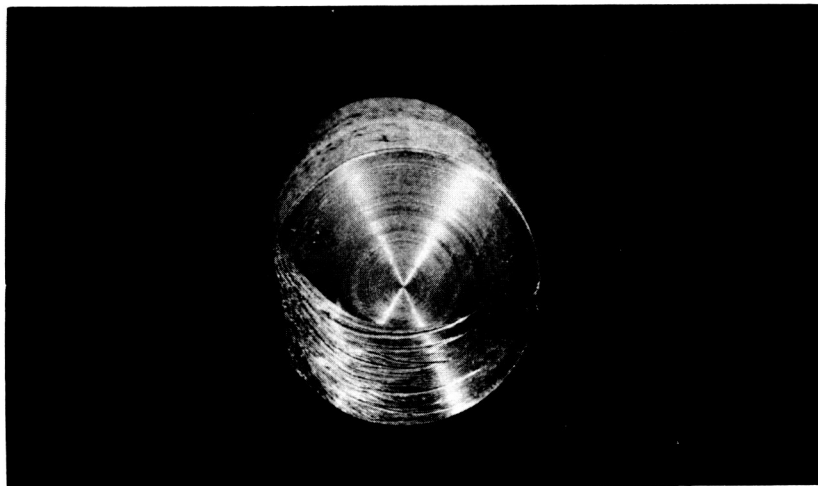
A difficulty common to all procedures investigated in the course of this program is that localized melting of the asperities apparently led immediately to microscopic welding between the contacting surfaces and to subsequent galling of the surfaces. It can, therefore, be theorized that to achieve a successful plateauing technique, the contacting surfaces must have a high resistance to being welded together.

Another difficulty arises out of the requirement for precise positioning of the surfaces. If a surface having an initial roughness of, say, 16 microinches, is to be "plateaued", the resulting flats would have to have surface



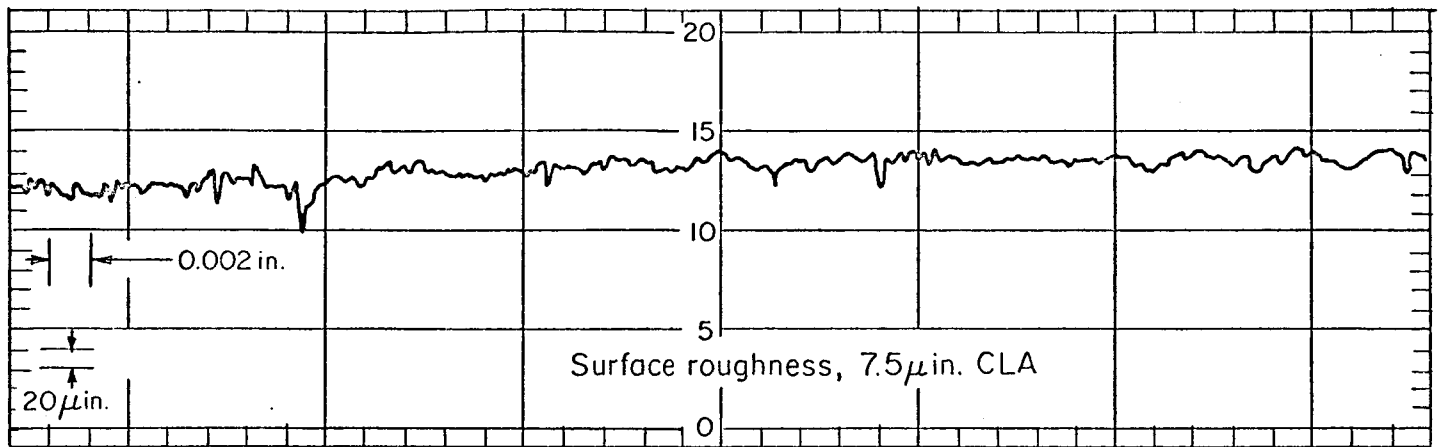
35565

FIGURE 14. GALLING AND PITTING DAMAGE OF ALUMINUM SURFACES CAUSED BY RELATIVE MOTION WITH ELECTRIC CURRENT PULSE HEATING, WITH SPECIMEN SURFACES DRY

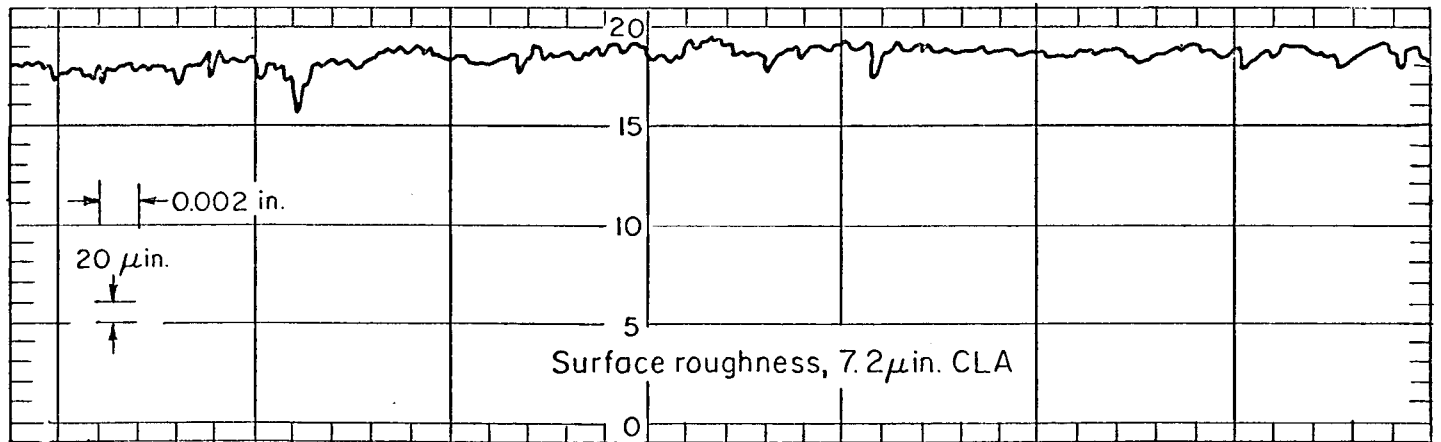


35566

FIGURE 15. GALLING AND PITTING DAMAGE OF ALUMINUM AND STAINLESS STEEL SURFACES CAUSED BY RELATIVE MOTION WITH ELECTRIC CURRENT PULSE HEATING, WITH SPECIMEN SURFACES DRY



a. Before Surface Treatment



b. After Surface Treatment

FIGURE 16. TALYSURF CHARTS SHOWING APPARENT SLIGHT SMOOTHING EFFECT OF ELECTRIC CURRENT PULSE HEATING AN ALUMINUM SURFACE WITH A PRESSED GRAPHITE TOOL

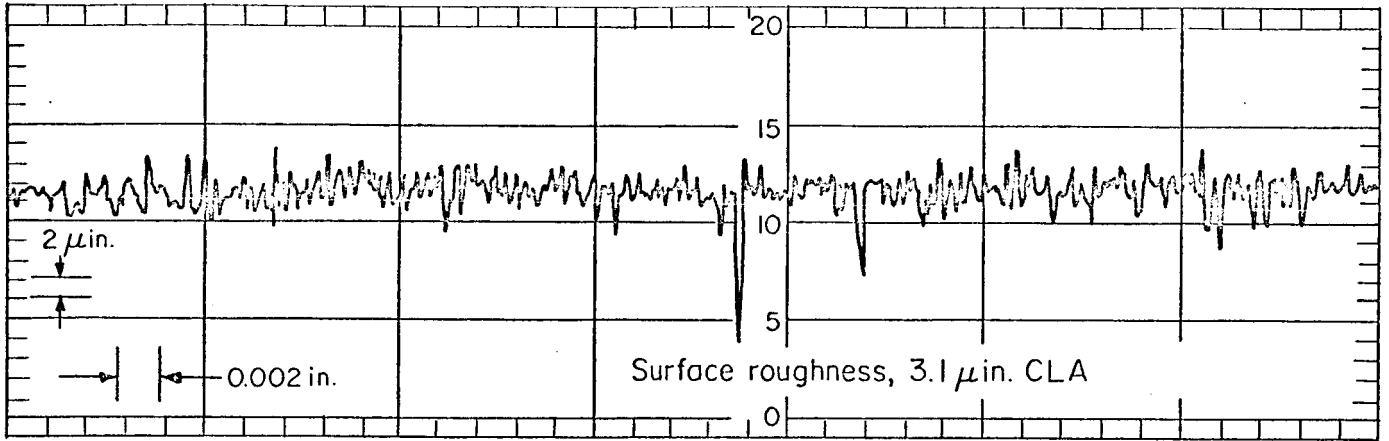


FIGURE 1 . TALYSURF CHART SHOWING ALUMINUM SURFACE LAPPED WITH A FINE-GRIT COMPOUND

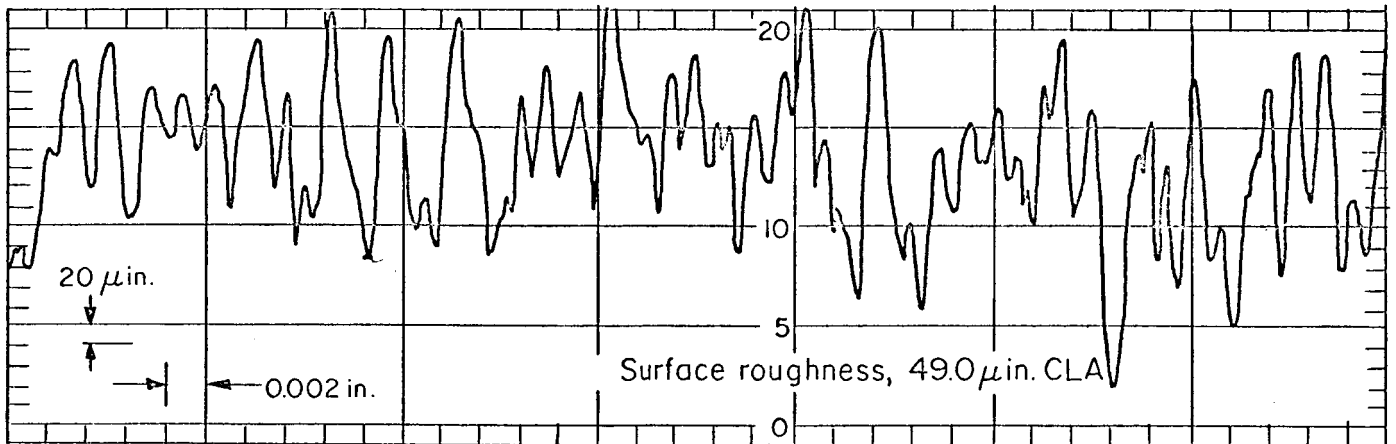


FIGURE 18. TALYSURF CHART SHOWING ELECTRIC DISCHARGE MACHINED MILD-STEEL SURFACE

roughnesses of a fraction of a microinch in order to fit the general picture of a plateaued surface. To achieve this by relative motion between two surfaces, the planes of translation or axes of rotation must remain true within a fraction of a microinch. This type of precision in positioning is not attainable with any ordinary or even extraordinary types of machine tools. It is probable, therefore, that one of the surfaces would have to be a small "slipper" that would, in effect, span the peaks of no more than several asperities at a time.

Because the flat portions of any plateaued surface will still have surface asperities of some size, an obvious final consideration is the scale of plateauing that must be achieved to increase the thermal contact between mating surfaces.

When it is considered that thermal energy is manifested in metallic solids by crystal-lattice vibrations and the motion of an electron "cloud", according to current theory, it can be reasoned that two surfaces in contact conduct heat directly at locations where the spacing between the surfaces is on the same order as the atomic spacing of the crystal lattices, or at least within the range of separation at which intermolecular forces have significant effect.

An investigation of this consideration was outside the scope of the program; nevertheless, it appears to be a consideration of prime importance to this program.

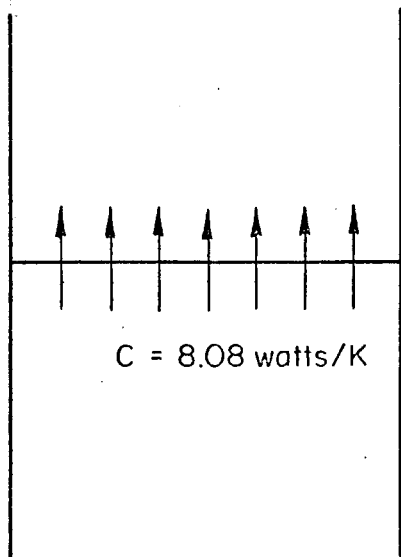
Diaphragm Effectiveness

As requested by Electro-Mechanical Engineering personnel at Huntsville, Alabama, calculations were performed to predict the effectiveness of the diaphragm on the flexible-surface test specimen in conducting heat. The derivation of an expression and the resulting computations are presented in Appendix B.

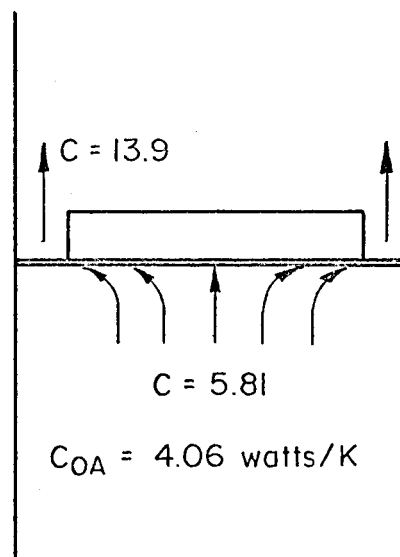
As would be expected, the effectiveness is a function of the conductance coefficient of the interface between the diaphragm and the rigid member. From Reference (5), it appears that a conductance coefficient of about 5,000 Btu/hr-ft²-F (about 3 watts/cm²-K) is attainable with an ordinary machined joint; assuming the conductance coefficient can be improved by a factor of 10 by the effect of the diaphragm and surface treatment gives us a value of 50,000 Btu/hr-ft²-F. With the flexible-surface-specimen design, the diaphragm thickness is 0.026 inch and the diameter is 0.75 inch; for this geometry and the high conductance-coefficient value, the computed effectiveness of the diaphragm is 7.2 percent.

Figure 19 illustrates the significance of this low conductance.

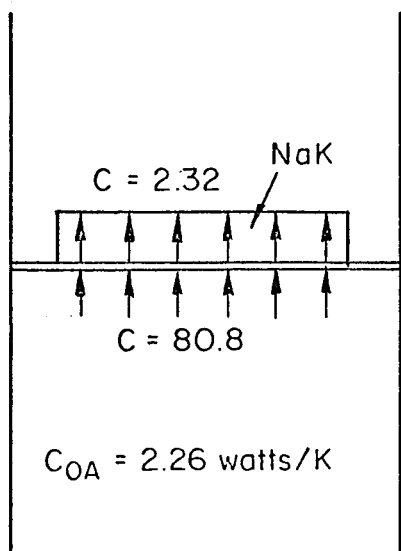
The overall conductance of an ordinary rigid-rigid joint with an interface h of 5,000 Btu/hr-ft²-F is 8.08 watts/K. The conductance of the diaphragm



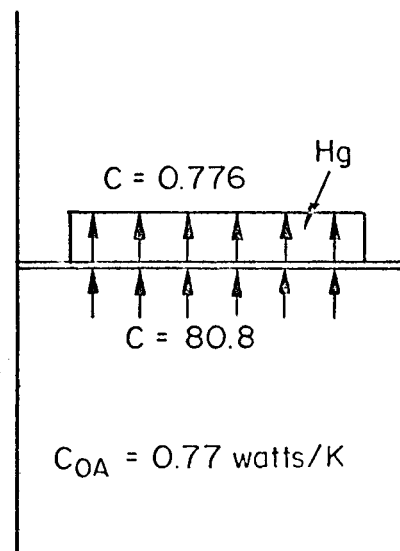
a) Ordinary joint
 $h = 5000 \text{ Btu/hr-sq ft (F)}$



b) Diaphragm joint, no
 fluid conductance
 $h = 50,000 \text{ Btu/hr-sq ft (F)}$



c) Diaphragm joint,
 NaK fluid
 $h = 50,000 \text{ Btu/hr-sq ft (F)}$



d) Diaphragm joint,
 mercury fluid
 $h = 50,000 \text{ Btu/hr-sq ft (F)}$

FIGURE 19. OVERALL CONDUCTANCE OF ORDINARY RIGID-SURFACE JOINT AND TYPICAL DIAPHRAGM JOINTS

with an h of 50,000 Btu/hr-ft²-F is 5.81 watts/K in series with the rim conductance of 162 watts/K--giving an overall conductance of 4.06 watts/K, or about one-half the conductance of the ordinary joint.

Considering the conductance of the fluid pocket separately, assuming the pocket is 0.125 inch deep, the overall conductance of the joint is 2.26 watts/K with NaK and 0.77 watts/K with mercury. To break even with the ordinary joint, the depth of the pocket (with NaK) would have to be on the order of 0.030 inch. This pocket depth should be mechanically satisfactory, but very little reduction beyond this can be considered without getting into mechanical problems.

If the action of the conductive paste and the diaphragm-rim combination together is considered, it is necessary to assume that the presence of the paste tends to even out the temperature distribution in the diaphragm, thus reducing the proportion of heat going into the rim; therefore, one cannot superimpose the conductance of the diaphragm alone and the fluid alone to obtain the effective conductance of the combination.

If an ordinary joint with an h of 1,000 Btu/hr-ft²-F is compared with a diaphragm joint with an h of 10,000 Btu/hr-ft²-F, the comparison is more favorable. The effectiveness of the diaphragm is about 16 percent and the conductance of the diaphragm joint is 2.18 watts/K as contrasted to 1.61 watts/K for the ordinary joint. However, this is still only a 25 percent increase in overall conductance.

The results of this analysis indicate that only a limited improvement in overall joint conductance can be achieved at best, even if a tenfold increase in interface conductance is achieved.

* * * * *

Information upon which this report is based may be found in Battelle Laboratory Record Book Number 23499.

CLC/FAC/JES:mvv

REFERENCES

- (1) Jakob, M., and Hawkins, G. A., Elements of Heat Transfer, Third Edition, John Wiley and Sons, Inc., New York (1957).
- (2) Shurig, O. R., "How Should Engineers Describe a Surface", Proceedings of The Special Summer Conference on Friction and Surface Finish held at the Massachusetts Institute of Technology, Cambridge, Massachusetts, 141-156 (June, 1940).
- (3) Wallace, D. A., "The Preparation of Smooth Surfaces", Proceedings of the Special Summer Conference on Friction and Surface Finish held at the Massachusetts Institute of Technology, Cambridge, Massachusetts, 22-43 (June, 1940).
- (4) Spear, P., and Robinson, I. R., "The Influence of Machining and Grinding Methods on the Mechanical and Physical Condition of Metal Surfaces", Institute of Metals Monograph and Report Series No. 13, 59-100 (1953).
- (5) Kasperek, W. E., and Dailey, R. M., "Measurements of Thermal-Contact Conductance Between Dissimilar Metals in a Vacuum", ASME Paper No. 64-HT-38 (August, 1964).
- (6) Bowden, F. P., and Tabor, D., The Friction and Lubrication of Solids, The University Press, Oxford (1954).
- (7) Schneider, P. J., Conduction Heat Transfer, Addison-Wesley Publishing Co., Inc., Reading, Massachusetts (1957).

BIBLIOGRAPHY

"Engineering Guide to Silicone Fluids", Dow Corning Corporation (1958).

Bowden, F. P., and Tabor, D., "The Influence of Surface Films on the Friction and Deformation of Surfaces", Institute of Metals Monograph and Report Series No. 13, 197-212 (1953).

Way, S., "Description and Observation of Metal Surfaces", Proceedings of the Special Summer Conference on Friction and Surface Finish held at the Massachusetts Institute of Technology, Cambridge, Massachusetts, 44-75 (1940).

"NaK - The Liquid Metal for Practical High Temperature Heat Transfer Systems", Bulletin HT-1-761, MSA Research Corporation, Callery, Pennsylvania.

"Surface Roughness, Waviness and Lay, American Standard", Published by The American Society of Mechanical Engineers, New York (1955).

Greenwood, J. A., "On Area of Contact Between Rough Surfaces and Flats", ASME Paper No. 65-Lub-10 (October, 1965).

Peklenik, J., "Contribution to the Theory of Surface Characterization", Paper presented at the International Institution for Production Engineering Research (CIRP), Cincinnati (September, 1963).

Westwood, A. R. C., "Surface Sensitive Mechanical Properties", I & EC 56:14-25 (September, 1964).

Williamson, J. P. B., "Dependence of the Reliability of Electrical Connections and Joints on the Microtopography of the Mating Surfaces", Mach. Des. 36:1724 (May 7, 1964).

Cocks, M., "Role of the Displaced Metal in the Sliding of Flat Metal Surfaces". J. Ap. Phys. 35:1807 (June, 1964).

Cocks, M., "Interaction of Sliding Metal Surfaces", J. Ap. Phys. 33:2152-61 (July, 1962).

"Properties of Metallic Surfaces: Symposium", Metal Prog. 80:126 + (November, 1961).

Barwell, F. T., "Surface Contact in Theory and Practice", Inst. Mech. Eng. Proc. 175 No. 17: 853-76, Discussion 876-8.

Thompson, J. E., and Turner, M. J. B., "Wear of Graphite Sliding on a Steel Surface and the Influence of an Electric Current on the Rate of Wear", Inst. E. E. Proc. 109A: 235-42 (June, 1962).

Seekins, H. L., "Evaluating Surface Finishes", I.S.A. J 10:51-6 (February, 1963).

BIBLIOGRAPHY (Continued)

- Chandiramani, K. L., and Cook, N. H., "Investigations on the Nature of Surface Finish and Its Variation with Cutting Speed", ASME Trans. (B) 86:134-40 (May, 1964).
- Bennett, H. E., "Measurement of Smooth Surface Finishes", Ind. Qual. Control 20:18-23 (February, 1964).
- Bryan, J. B., et al., "Measuring Surface Finish; State-of-the-Art Report", Mech. Eng. 85:42-6 (December, 1963).
- "World Manufacturing Research; CIRP Meeting", Cincinnati: Abstracts of Papers on Surface Finishes. Tool & Mfg. Eng. 53:65-8 (July, 1964).
- Hagstrum, H. D., "Surfaces of Solids", Bell Lab Rec. 40:282-8 (September, 1962).
- Davis, M. G., "Generation of Pressure Between Rough, Fluid Lubricated, Moving, Deformable Surfaces", Lub. Eng. 19:246-52 (June, 1963).
- Witzke, F. W., "How to Control Surface Textures of Machine Parts", Mag. of Stand. 34:50-1 (February, 1963).
- "Film Unveils Surface Roughness", Iron Age 192:106 (September 19, 1963).
- "Surface Finish Metrology", Automobile Eng. 53:325 (July, 1963).
- "Surface Texture" Reference Book Sheet, Am. Mach/Metalworking Mfg. 107:125 (April 15, 1963).
- Bourne, H. L., "Silicon Monoxide Technique for Observing Surface Microtopography", Am. Cer. Soc. J. 99:53-4 (January, 1966).
- "Finish Measurement", Mach. 71:187 (August, 1965).
- Eberhard, H. W., "How Rough the Surface"? Prod. Eng. 36:105-7 (August 16, 1965).
- "Instruments for Surface Measurement", Engineer 220:26 (July 2, 1965).
- "Mechanical Surface-Roughness Indicator", Engineer 220:469 (September 17, 1965).
- Gabe, D. R., "Methods of Measuring Surface Roughness", Metallurgia 72:47-52 (July, 1965).
- Robinowicz, E., "Surface Energy Approach to Friction and Wear", Product Eng. 36:95-9 (March 15, 1965).
- Williams, K., and Giffen, E., "Friction Between Unlubricated Steel Surfaces at Sliding Speeds up to 750 Ft/Sec", Inst. Mech. Eng. Proc. 178 pt 3N:24-36 .

BIBLIOGRAPHY (Continued)

Glaeser, W. A., "Wear and Friction of Solid Surfaces", Metal Prog. 87:146 + (April, 1965).

Kubo, M., "Instrument for the Measurement of Slope and Height Distribution of Surface Roughness", R. Sci. Instr. 36:236-7 (February, 1965).

APPENDIX A

FLEXIBLE SURFACE DIAPHRAGM THICKNESS,
EQUATION DERIVATION AND DESIGN COMPUTATION

APPENDIX A

FLEXIBLE SURFACE DIAPHRAGM THICKNESS, EQUATION DERIVATION AND DESIGN COMPUTATION

The flexibility of the diaphragm is a function of both the modulus of elasticity (E) of the material and the thickness of the diaphragm. In order to obtain the expression for the pressure required to cause a diaphragm of thickness (t) to conform to a surface with waviness of a wavelength λ and peak-to-peak amplitude δ , it is assumed that the surface waviness can be expressed as a cosine function. That is,

$$y = \frac{\delta}{2} \left[\cos \left(\frac{x}{\lambda} 2\pi \right) - 1 \right] \quad (\text{A-1})$$

where y is the vertical distance measured from the peaks. That is,

$$\begin{aligned} \text{at } x = \lambda & \quad y = 0, \\ \text{and at } x = \lambda/2, & \quad y = -\delta. \end{aligned}$$

Now y is also the required deflection of the diaphragm (it is also assumed that the problem can be considered to be two dimensional).

Now the loading (p) on the diaphragm required to produce the deflection as expressed by Equation (A-1) is,

$$p = EI \frac{d^4 y}{dx^4} \quad (\text{A-2})$$

where I is the moment of inertia of the diaphragm section. Working within 1 wave length and combining Equations (A-1) and (A-2) gives

$$p = \frac{EI\delta}{2} \left(\frac{2\pi}{\lambda} \right)^4 \cos \left(\frac{x}{\lambda} 2\pi \right). \quad (\text{A-3})$$

This equation implies that the loading to produce the required deflection is also a cosine function, zero at the peaks and maximum at the valleys. However, for this case, any loading that is at least as great at any point as that from Equation (A-3) will produce the required deflection. Therefore,

$$P_{\max} = P = EI\delta \left(\frac{\pi}{\lambda} \right)^4 \quad (\text{A-4})$$

where P is the required uniform pressure. For a unit strip of the diaphragm of thickness t,

$$I = \frac{t^3}{12} .$$

Therefore,

$$P = \frac{Et^3 \delta 8\pi^4}{12\lambda^4}$$

or

$$\frac{P}{Et^3} = \frac{65 \delta}{\lambda^4} \quad (A-5)$$

Equation (A-5) is then used to determine the required thickness for the flexible-surface diaphragm.

The preliminary design computations for the flexible surface diaphragm that was proposed for the experimental portion of this study are as follows. From the surface model shown in Figure 7,

Waviness amplitude (peak-to-valley displacement),

$$\delta = 7.0 \times 10^{-4} \text{ inches.}$$

Waviness wavelength, $\lambda = 0.30$ inch.

From Equation (A-5),

$$\frac{P}{Et^3} = \frac{65 \delta}{\lambda^4}$$

$$\frac{P}{t^3} = \frac{65\delta E}{\lambda^4} = \frac{(65)(7.0 \times 10^{-4} \text{ in.})(10 \times 10^6 \text{ lb/in.}^2)}{(0.3 \text{ in.})^4}$$

$$= \frac{455 \times 10^3 \text{ lb/in.}}{81 \times 10^{-4} \text{ in.}^4}$$

$$\frac{P}{t^3} = 5.62 \times 10^7 \text{ lb/in.}^5$$

$$t^3 = \frac{(P \times 10^{-7})(10^{-2})}{5.62 \times 10^{-2}} \text{ in.}^3 \quad t = 10^{-3}(P/0.0562)^{1/3} \text{ in.}$$

For $P = 1000$ psi,

$$t = 10^{-3} (1000/0.0562)^{1/3} \text{ in.}$$

$$t = 10^{-3} (17,800)^{1/3} \text{ in.}$$

$$t = 10^{-3} \times 26.1 = 0.0261 \text{ in.}$$

$$t = 0.026 \text{ in.}$$

APPENDIX B

EFFECTIVENESS OF DIAPHRAGM IN TRANSFERRING
HEAT, NEGLECTING THE CONDUCTANCE OF THE
PRESSURIZING HYDROSTATIC FLUID OR PASTE,
EQUATION DERIVATION AND EXAMPLE COMPUTATION

APPENDIX B

EFFECTIVENESS OF DIAPHRAGM IN TRANSFERRING HEAT,
NEGLECTING THE CONDUCTANCE OF THE PRESSURIZING HYDROSTATIC FLUID OR PASTE
EQUATION DERIVATION AND EXAMPLE COMPUTATION

Heat balance on radial element of diaphragm:

$$- \frac{dq_k}{dr} \Delta r + \Delta q_h = 0 . \quad (B-1)$$

Now

$$q_k = - k \ 2\pi r \ t \ \frac{dT}{dr} . \quad (B-2)$$

Differentiating gives

$$\begin{aligned} \frac{dq_k}{dr} &= - 2\pi k t \ \frac{d}{dr} \left(r \frac{dT}{dr} \right) \\ &= - 2\pi k t \left(r \frac{d^2 T}{dr^2} + \frac{dT}{dr} \right) . \end{aligned} \quad (B-3)$$

Heat transferred across diaphragm surface:

$$\Delta q_h = -h \cdot 2\pi r \cdot T \Delta r \quad (B-4)$$

Substituting (B-3) and (B-4) in (B-1) gives

$$2\pi k t \left(r \frac{d^2 T}{dr^2} + \frac{dT}{dr} \right) \Delta r - 2\pi h T r \Delta r = 0 ,$$

which simplifies to

$$r^2 \frac{d^2 T}{dr^2} + r \frac{dT}{dr} - \frac{h}{kt} r^2 T = 0 . \quad (B-5)$$

Now let $\frac{h}{kt} = N^2$ (B-6)

and substitute in (B-5):

$$r^2 \frac{d^2 T}{dr^2} + r \frac{dT}{dr} - N^2 r^2 T = 0 . \quad (B-7)$$

From Reference (7)

$$T = C_1 J_0(iNr) + C_2 Y_0(iNr), \quad (B-8)$$

where $J_0(iNr)$ is the zero-order bessel function of the first kind and Y_0 is the zero-order bessel function of the second kind.

The boundary conditions are

$$T = T_0 \quad \Delta T \quad r = r_0 \quad (B-9)$$

$$\frac{dT}{dr} = 0 \quad \text{at } r = 0 \quad (B-10)$$

First B.C.:

$$T_0 = C_1 J_0(iNr_0) + C_2 Y_0(iNr_0). \quad (B-11)$$

Second B.C.:

$$J_0'(x) = -J_1(x) \quad (B-12)$$

$$\frac{d}{dr} [J_0(iNr)] = -iN J_1(iNr). \quad (B-13)$$

Similarly

$$\frac{d}{dr} [Y_0(iNr)] = -iN Y_1(iNr). \quad (B-14)$$

Substituting,

$$0 = C_1 iN J_1(0) - C_2 iN Y_1(0). \quad (B-15)$$

Now $J_1(0) = 0$ and $Y_1(0) = -\infty$

Therefore, $C_2 = 0$.

$$T_0 = C_1 J_0(iNr_0) \quad (B-16)$$

$$C_1 = \frac{T_0}{J_0(iNr_0)}. \quad (B-17)$$

Substituting (B-15) and (B-17) into (B-11):

$$T = T_0 \frac{J_0(iNr)}{J_0(iNr_0)}. \quad (B-18)$$

Now the heat entering the rim is

$$q_r = -2\pi k r_o \frac{dT}{dr} \quad (B-19)$$

Differentiating (B-18):

$$\frac{dT}{dr} = \frac{T_o}{J_o(iNr_o)} \left[-iN J_1(iNr) \right] \quad (B-20)$$

And substituting in (B-19):

$$q_r = -2\pi k r_o t T_o \frac{[-iN J_1(iNr_o)]}{J_o(iNr_o)} \quad (B-21)$$

Now the ideal heat input is

$$q_{ideal} = -h\pi r_o^2 T_o \quad (B-22)$$

The effectiveness of the diaphragm is defined as

$$\eta = \frac{q_r}{q_{ideal}} \quad (B-23)$$

$$\eta = \frac{2\pi k r_o t T_o [-iN J_1(iNr_o)]}{-h\pi r_o^2 T_o J_o(iNr_o)} \quad (B-24)$$

$$\eta = \frac{2i J_1(iNr)}{Nr_o J_o(iNr_o)} \quad (B-25)$$

Now using the modified bessel function,

$$I_n(x) = i^{-n} J_n(ix) \quad (B-26)$$

Yields

$$I_o(x) = J_o(ix) \quad (B-27)$$

and

$$I_1(x) = i^{-1} J_1(ix) = -i J_1(ix) \quad (B-28)$$

or

$$\eta = \frac{2I_1(Nr_o)}{Nr_o I_o(Nr_o)} \quad (B-29)$$

Let $r_o = 0.75$ in.

$k = 115$ Btu/hr-ft-F

$t = 0.026$ in.

$A = \frac{\pi}{4} \left(\frac{75}{12} \right)^2 = 0.00306$ ft²

$$N = \sqrt{\frac{h}{kt}} = \sqrt{\frac{h}{115 (0.026)}} = \sqrt{4.01 h}$$

$$Nr_o = \sqrt{4.01 h} \frac{0.75}{12} = 0.125 \sqrt{h}$$

TABLE B-1. DIAPHRAGM EFFECTIVENESS VALUES FOR SELECTED VALUES OF JOINT CONDUCTANCE COEFFICIENT

$\frac{h,}{\text{hr-ft}^2\text{-F}}$	\sqrt{h}	Nr_o	η	$\frac{hA,}{\text{hr-F}}$	$\frac{\eta hA,}{\text{hr-F}}$	$\frac{\eta hA,}{\text{watts}}$
$\frac{\text{Btu}}{\text{hr-ft}^2\text{-F}}$						K
100	10	1.25	0.845	0.306	0.258	0.136
1,000	31.6	3.95	0.436	3.06	1.33	0.703
5,000	70.7	8.84	0.226	15.3	3.46	1.83
10,000	100	12.5	0.160	30.6	4.90	2.59
50,000	224	28.0	0.072	153	11.0	5.81
100,000	316	39.5	0.051	306	15.5	8.19

Conductance of rim:

$$C_{\text{rim}} = \frac{kA}{L} = \frac{115\pi(0.875)(0.125)}{0.125 (12)} = 26.3 \frac{\text{Btu}}{\text{hr F}}$$

$$= 13.9 \text{ watts/K} .$$

Conductance of fluid pocket:

$$C = \frac{kA}{L} = k \frac{(0.00306) 12}{(0.125)} = 0.294 k$$

TABLE B-2. FLUID-POCKET CONDUCTANCE VALUES FOR
SELECTED HYDROSTATIC FLUIDS

Fluid	k, Btu/hr-ft-F	C, Btu/hr-F	C, watts/K
NaK	15	4.40	2.32
Hg	5	1.47	0.776
Silicone + metal powder	0.4	0.12	0.0633
Silicone	0.01	0.002	0.00106

NOMENCLATURE

English Letters

A	heat-transfer area
C	constant or coefficient
E	material modulus of elasticity
I	section moment of inertia
N	parameter, $\sqrt{h/Kt}$
P	pressure
T	temperature
h	interface conductance coefficient
k	thermal conductivity
p	diaphragm loading
q	heat-transfer rate
q'	heat-transfer rate per unit length
r	radius
t	diaphragm thickness
x	arbitrary parameter
y	vertical distance from surface peaks

Greek Letters

Δ	increment
δ	maximum distance from peak to valley on surface amplitude
η	diaphragm effectiveness
λ	maximum distance between surface peaks (wavelength)

Mathematical Notation

i	$\sqrt{-1}$
$I_n(x)$	modified Bessel function
$J_n(x)$	Bessel function of first kind
$Y_n(x)$	Bessel function of second kind

NOMENCLATURE (Continued)

Subscripts

- h heat entering diaphragm surface
- k heat flow by conduction in diaphragm
- o diaphragm or outer
- i inner